Transcriptional responses of *Escherichia coli* during recovery from inorganic or organic mercury exposure

Stephen LaVoie (slavoie5@uga.edu) and Anne O. Summers* (summers@uga.edu)

Department of Microbiology, University of Georgia, Athens, Georgia 30602

Keywords: longitudinal RNA-Seq, transcriptomics, toxic metals, essential metals, stress response, biofilm, phenylmercury, antibiotic resistance

ABSTRACT

Background: The protean chemical properties of mercury have long made it attractive for diverse applications, but its toxicity requires great care in its use, disposal, and recycling. Mercury occurs in multiple chemical forms, and the molecular basis for the distinct toxicity of its various forms is only partly understood. Global transcriptomics applied over time can reveal how a cell recognizes a toxicant and what cellular subsystems it marshals to repair and recover from the damage. The longitudinal effects on the transcriptome of exponential phase *E. coli* were compared during sub-acute exposure to mercuric chloride ($HgCl_2$) or to phenylmercuric acetate (PMA) using RNA-Seq.

Results: Differential gene expression revealed common and distinct responses to the mercurials throughout recovery. Cultures exhibited growth stasis immediately after each mercurial exposure but returned to normal growth more quickly after PMA exposure than after $HgCl_2$ exposure. Correspondingly, PMA rapidly elicited up-regulation of a large number of genes which continued for 30 min, whereas fewer genes were up-regulated early after $HgCl_2$ exposure only some of which overlapped with PMA up-regulated genes. By 60 min gene expression in PMA-exposed cells was almost indistinguishable from unexposed cells, but $HgCl_2$ exposed cells still had many differentially expressed genes. Relative expression of energy production and most metabolite uptake pathways declined with both compounds, but nearly all stress response systems were up-regulated by one or the other mercurial during recovery.

Conclusions: Sub-acute exposure influenced expression of ~45% of all genes with many distinct responses for each compound, reflecting differential biochemical damage

by each mercurial and the corresponding resources available for repair. This study is the first global, high-resolution view of the transcriptional responses to any common toxicant in a prokaryotic model system from exposure to recovery of active growth. The responses provoked by these two mercurials in this model bacterium also provide insights about how higher organisms may respond to these ubiquitous metal toxicants.

BACKGROUND

The common metallic element mercury (Hg) has no beneficial biological function and its chemical similarities to essential transition metals such as zinc, copper, and iron make it highly toxic to all living systems. Global mercury emissions range from 6500 to 8500 Mg annually with estimates of half [1, 2] and even two-thirds [3] being anthropogenic and the rest from volcanism. Mercury exists in multiple chemical forms that are readily susceptible to abiotic and biotic inter-conversions [4]. Mercury occurs naturally as the insoluble HgS ore (cinnabar), as inorganic complexes of Hg^{+2}, Hg^{+1}, or $(Hg_2)^{2+}$ of varying solubility depending on available ligands, and as organomercurials generated by microbial and anthropogenic processes.

Major sources of chronic mercury exposure in humans include dental amalgam fillings [5, 6], consumption of fish containing methylmercury [7], and artisanal gold mining operations [8]. Organomercurials, like phenylmercury, methylmercury, and merthiolate (ethylmercury) have historically been used in medical, industrial and agricultural applications as antimicrobial or fungicidal agents [9-11]. The toxic effects of mercury exposure in humans are associated with neurological, kidney, liver, gastrointestinal, and developmental disorders [9, 12-15].

Like other common electrophilic toxic metals such as arsenic, cadmium, and lead, there is no single biochemical target for mercury damage. Mercury has a strong affinity for sulfur and selenium [16, 17] and therefore targets the cellular thiol pool, composed of glutathione and cysteine thiol groups of proteins [9] and selenocysteine, a rare but critical amino acid in proteins involved in redox defense and thyroid function [18]. Depletion of the cellular thiol pool and disruption of the cellular membrane potential by mercury can induce oxidative stress and apoptosis pathways in mitochondria [19, 20]. However, there is no evidence that mercury itself undergoes Fenton-type chemistry to generate reactive oxygen species like iron and copper [21].

In earlier work we used global proteomics to identify stable mercury-protein binding sites in growing *E. coli* cells exposed to acute levels of organic or inorganic Hg [22]. We found cysteine sites in several hundred proteins, many highly conserved evolutionarily, that formed stable adducts with one or more of these mercurials, consequently disrupting many cellular processes such as iron homeostasis and the electrolyte balance [23]. Importantly, we found that organic and inorganic mercurials had distinct effects on these cellular processes and distinct protein structural preferences. Although the pathobiology of organic and inorganic mercurials has been known for decades to differ, with methyl- and ethyl-mercury recognized as neurotoxic and inorganic mercury as neurotoxic, nephrotoxic, hepatotoxic, and immunotoxic, no previous studies at that time had assessed the biochemical underpinnings of these distinctions on a global scale in any model system.

Motivated by our proteomics observations and by microarray data from *C. elegans* showing distinct transcriptional single end point response and toxicity for

inorganic and organic mercurials [24], we applied RNA-Seq to examine the transcriptional effects of $HgCl_2$ and phenylmercuric acetate (PMA) exposure on *E. coli* K-12 MG1655 over time. This is the first study to examine the global transcriptional response to mercury exposure in a microorganism and the only study to compare directly the effects of different compounds over time through recovery. The changes in gene expression were idiosyncratic for each compound, confirming and extending the idea that the cell suffers overlapping but distinct biochemical damage and marshals both distinct and overlapping recovery processes in response to these chemically distinct mercurials. Although our work was in a bacterium, the high evolutionary conservation of many of the genes whose expression we identified as mercury-vulnerable offers insights for the toxicology of mercury compounds in higher organisms.

METHODS

Cell cultures.

For each biological RNA-Seq replicate *E coli* K-12 MG1655 was subcultured from cryostorage on Luria-Bertani (LB) agar overnight at 37°C. A half-dozen well-isolated colonies were used to inoculate a 20 ml starter culture in Neidhardt MOPS Minimal Medium (NM3) [25] (0.2% final glucose concentration) supplemented with 20 mg/L uracil and 500 µg/L thiamine, which was incubated at 37°C with shaking at 250 rpm overnight (~18 hr). The overnight starter culture was diluted 1:30 to initiate the experimental culture and divided into three 500 ml flasks with 100 ml NM3 in each, which were incubated at 37°C with shaking at 250 rpm. When cultures reached $OD_{595} \approx 0.470$ (~ 200 min), two cultures were made 3 µM mercuric chloride ($HgCl_2$) or 3 µM

116 phenylmercuric acetate (PMA) and the third was left as an unexposed control. Mercury
117 stocks were prepared fresh for each growth experiment: 10 mM $HgCl_2$ (Fisher) in water
118 and 5 mM PMA (Sigma) in 25% dimethyl sulfoxide DMSO (Fisher), which is 2.1 mM or
119 0.015% v/v final concentration DMSO in culture. These mercurial exposures were
120 chosen from prior pilot experiments to find exposure conditions (OD_{595}, mercurial
121 concentration and sampling times) that displayed a marked decrease in growth rate
122 relative to the unexposed control but allowed subsequent restoration of rapid growth
123 rate (i.e. recovery) within 1 hr (approximately one generation in NM3) after mercurial
124 exposure. Duplicate 1-ml aliquots of each culture were collected at 0 (unexposed
125 control only), 10, 30, 60 min after mercurial exposure and immediately centrifuged at
126 20,800 *x g* for 3 min at 4°C. Spent medium was aspirated and cell pellets were frozen at
127 -70°C within 5 min after collection. Seven biological replicates were prepared following
128 this protocol and the average variance for all replicates in culture optical density over
129 each 90-min experiment ranged from 0.0019 – 0.0073. The three biological replicates
130 with the lowest variance between growth curves (range from 0.0007 – 0.0017 for all
131 time points) were prepared for RNA-Seq.
132
133 ***Purification of mRNA***
134 One cell pellet from each condition and sampling time was thawed on ice for all
135 three biological replicates; total RNA was isolated by RNA*snap*™ [26] and stored at -
136 70°C. DNA contamination was removed by two treatments with Turbo-DNase (Ambion;
137 Life Technologies). RNA concentrations and A_{260}/A_{280} ratios were determined using a
138 Nanodrop™ 1000 spectrophotometer (Thermo Scientific). Ribosomal RNA depletion was

139 performed with the Ribo-Zero™ rRNA removal kit for Gram-negative bacteria (Epicentre)
140 and concentrated using RNA Clean and Concentrator™ -5 columns (Zymo Research)
141 following the manufacturer's instructions. Purified mRNA was quantified using the
142 Nanodrop™ and stored at -70°C.
143
144 ***Library Preparation and Next-generation Sequencing***
145 The quality and quantity of rRNA-depleted RNA was assessed on a 2100
146 Bioanalyzer RNA pico chip (Agilent Technologies) using the manufacturer's
147 recommendations. Next-generation sequencing (NGS) libraries were prepared using the
148 Kapa biosystems NGS stranded library prep kit for RNA-Seq with dual indexed Illumina
149 adapters. Library insert size was ~150 bp, as determined by high-sensitivity NGS
150 fragment analysis kit for Fragment Analyzer™ (Advanced Analytical Technologies) using
151 the manufacturer's instructions. Quantification of each library was done by qPCR and all
152 30 libraries were pooled in equal concentrations. The library preparation, quality
153 analysis, and pooling were performed by the Georgia Genomics Facility
154 (http://dna.uga.edu). Paired-end (2 x 50 bp) sequencing of the pooled libraries using the
155 Illumina HiSeq 2000 platform was performed by the HudsonAlpha Institute for
156 Biotechnology Genomic Services Laboratory (http://gsl.hudsonalpha.org). See Table S1
157 for index and filename information for data uploaded to NCBI Gene Expression
158 Omnibus database (http://www.ncbi.nlm.nih.gov/geo/) with accession ID: GSE95575.
159
160 ***Data Processing and Differential Expression Analysis***

Quality control processing of sequence data was performed using Galaxy (https://galaxyproject.org) on the Georgia Advanced Computing Resource Center at the University of Georgia. The FASTX tools in Galaxy (http://hannonlab.cshl.edu/fastx_toolkit) were used for filtering by quality (80% of sequence ≥ quality score of 20), then reads were trimmed at both 5' and 3' ends using a window and step size of 1 with quality score ≥ 20. Forward- and reverse-read mate-pairs were assembled and aligned to the *Escherichia coli* MG1655 K-12 genome using Bowtie2 [27]. SAMtools [28] was used to convert Bowtie2 output (.bam file) to SAM format. The number of sequence reads that aligned to features in the annotation file (Escherichia_coli_str_k_12_substr_mg1655.GCA_000005845.2.24.gtf from http://bacteria.ensembl.org) were tabulated from the resulting SAM alignment files using the HTSeq-count program [29] with intersection non-empty mode. Mapped read counts were analyzed for significant differential expression (false discovery rate of ≤ 0.01, fold-change ≥ 2) using the baySeq package in R [30]. All genes that did not meet both the ≤ 1% FDR and ≥ 2 fold-change criteria were indicated as no-change in figures, tables, and text. Within baySeq, two-way comparisons using quantile normalization were made for all three biological replicate transcriptomes over time for $HgCl_2$ exposure or PMA exposure versus the unexposed control. We also examined changes over time in the unexposed control culture itself.

RESULTS

Effects of sub-acute mercury exposure on growth of MG1655.

We defined sub-acute exposure as the concentration of mercury that clearly inhibited growth relative to the unexposed control but allowed cells to resume growth within 1 hour or approximately one generation in this medium (Figure 1a, Figure S1). We chose restoration of growth rate, not stationary phase cell density, as the benchmark for recovery so as not to conflate normal cellular stationary phase "stop growing" signals with mercury-induced "stop growing" signals. Based on pilot experiments the appropriate dose proved to be 3 μM for both mercurials. Exposure to 4 - 5 μM $HgCl_2$ prevented growth resumption during 1 hr and the effects of PMA exposure were similar at 3 and 5 μM; exposure to 2.5 μM of either mercurial did not consistently retard growth (data not shown).

Cell-associated Hg (Table S2 and Supporting Information Methods) declined slowly as has been reported previously for low level $HgCl_2$ exposure of Hg sensitive cells and was attributed to non-specific endogenous reductants [31-33]. Bound Hg in cells exposed either to $HgCl_2$ or to PMA declined similarly from ~50% of total Hg added to culture at 10 min to ~20% at 30 min, after which Hg loss from PMA-exposed cells continued to decline to 11% of input at 60 min. In contrast, cell-associated Hg in cells exposed to $HgCl_2$ increased from 24% at 30 to 47% at 60 min. Presently, we have no simple explanation for this unexpected difference in cell-bound Hg in late exponential phase cultures, however it does echo our finding that cultures acutely exposed to 40 μM or 80 μM PMA or $HgCl_2$ bound 24% or 208% more Hg(II) than PhHg, respectively [23]. Also notable was a brief drop in the culture optical density immediately after PMA exposure consistent with some cell lysis as has been reported [34]. The lack of

205 apparent lysis after divalent $HgCl_2$ exposure may be due to its ability to cross-link cell
206 envelope proteins via their cysteines, which is not possible for monovalent PMA.
207
208 ***Transcriptome benchmarks***
209 Paired-end libraries averaged over 9.5 million reads and mapped reads provided
210 an average of 143X coverage (Figure S2). The sequencing data were of high quality,
211 requiring removal of only 11% as low-quality reads. Of the high-quality reads, 97% of
212 reads mate-paired, 99.4% of paired reads mapped to the genome and 82% of reads
213 mapped to an annotated genome feature on average from all libraries.
214 Overall 89% of annotated mapped reads were to coding regions (CDS) based on
215 raw un-normalized read counts per gene output from HTseq-count program [29](Figure
216 S3, Table S3, Table S4). Pearson correlations of raw read counts confirmed that no
217 strong biases were introduced in biological replicates for each condition (Figures S4-
218 S6). That dispersion is slightly greater in both mercury exposure conditions than in
219 unexposed cultures, especially at later time points, is consistent with perturbations of
220 multiple cellular processes.
221 Mapped reads to rRNA constituted only 0.3% of total reads (std. dev. = 0.425) on
222 average for all libraries (Table S3) consistent with effective Ribo-Zero™ rRNA removal.
223 In the unexposed culture non-coding RNA's (ncRNA) were 4% of total reads over all
224 time points, but their percentage increased in mercury exposure conditions indicating
225 greater differential expression of some ncRNA genes (details below). The very
226 abundant tmRNA (*ssrA*) needed for rescuing stalled ribosomes [35] was 6% of total
227 reads in the unexposed condition and although this percentage increased for mercury

exposure conditions, the tmRNA gene (*ssrA*) was not differentially expressed under any condition. Pseudogenes accounted for less than 1% of total reads, but up to 35% ($HgCl_2$) and 13% (PMA) of them were significantly up-regulated. The tRNA's were less than 1% of total reads because the library preparation method we used was not optimized for such small RNAs. However, approximately 35% of these observed tRNA genes were significantly down-regulated during the first 30 min after exposure to either mercurial.

$HgCl_2$ and PMA transcriptional responses are not the same.

We expected that significantly differentially expressed genes (DEGs) in the mercury exposure conditions (compared to the unexposed cells) would change over time as the cells transitioned from initial growth stasis back into a normal growth rate. We also expected that some DEG responses would be similar because both mercurials are thiophilic and will bind to the cellular thiol redox buffer, glutathione (GSH), and to protein cysteine residues. However, since there are physiological differences and protein site preferences for each compound in acute Hg(II)- or PMA-exposure [23 and Zink et. al. in preparation] we aimed here at a low exposure using a longitudinal protocol to discern more subtle distinctions between these mercurials as the cells experienced stasis and then recovered their growth rate. In the following sections, we first describe the bulk measures of gene expression over time and then describe differences in specific functional pathways.

Differentially expressed genes: the view from 30,000 feet.

(a) Differentially expressed genes (DEG) for each condition and time point

DEGs were determined by pairwise comparisons of mercury exposure conditions relative to the unexposed culture at the corresponding time point (Figure 1b and Table S5). Ten minutes after exposure, expression of 41% or 49% of the 4,472 non-rRNA genes changed significantly for $HgCl_2$ or PMA-exposed cells, respectively (Figure 1b). At 30 min with growth still arrested, 32% of genes in the $HgCl_2$-exposed cells were differentially expressed (Figure 1b), (Figure 1a, red). In contrast, PMA-exposed cells at 30 min began to recover their prior growth rate (Figure 1a, green), but 45% of their genes remained differentially expressed (Figure 1b). By 60 min, the PMA-exposed cells were growing at nearly their pre-exposure rate and only 1.5% of genes were differentially expressed, whereas the $HgCl_2$-exposed cells were still growing more slowly than pre-exposure with 13% of their genes still differentially expressed compared to the unexposed cells (Figure 1b).

(b) Shared and unique genes at each time point for each exposure.

The total distinct DEGs across all time points was slightly lower for $HgCl_2$ (2,327) than for PMA (2,541) exposure (Figure 1b and Figure S7). More striking were the differences in DEGs at each time point; PMA-exposed cells modulated 20% more genes at 10 min (2,181 vs 1,821) and 40% more at 30 min (2,007 vs 1,422) than $HgCl_2$ exposed cells. This trend completely reversed by 60 min when DEGs declined in both exposure conditions but $HgCl_2$ exposed cells were still modulating ~9-fold more genes (563) than PMA-exposed cells (65), consistent with the latter recovering normal growth sooner (Figure 1a). Also notable is the carryover of DEGs from one time point to the

next where $HgCl_2$ exposed cells have 1,001 DEGs in common at 10 and 30 min after exposure but that number is 65% greater in PMA-exposed cells (1,650) (Figure S7). However, $HgCl_2$ exposed cells have 52% more DEGs that are unique at 10 min compared to PMA-exposed cells (804 vs 529), i.e. more $HgCl_2$ provoked DEGs occur sooner after exposure than later. $HgCl_2$ exposure also yields more DEGs that occur at all time points compared to PMA (Figure S7) since there are very few DEGs at 60 min for PMA exposure.

(c) Up-regulated vs. down-regulated genes for each exposure

Sorting expression simply into genes up-regulated or down-regulated by $HgCl_2$ or PMA at each time point (Figure 2) revealed additional quantitative distinctions between them. For up-regulated genes, PMA-provoked more unique DEGs than DEGs in common with $HgCl_2$ exposure at all time points, in contrast to $HgCl_2$ which had more DEGs in common than unique at all but the last time point. This trend was not continued for down-regulated genes where more genes were in common for both compounds than unique at all time points.

Thus, early in exposure the cell reduced expression of a similar number of genes for both mercurials, but up-regulated expression of many more genes in response to PMA than to $HgCl_2$, and these distinct trends persisted to the middle time point. By 60 min, gene expression of PMA-exposed cells closely resembled that of unexposed cells, but $HgCl_2$ exposed cells still have many up- and down-DEGs, consistent with slower growth rate recovery by $HgCl_2$ exposed compared to PMA-exposed cells (Figure 1a).

297 *(d) Differentially expressed genes grouped by functional category.*

298 To sort our observations from a different perspective, the DEGs for each
299 condition were grouped by Clusters of Orthologous Groups (COGs) to identify
300 expression differences based on gene functions (Figure 3 and Table S6). For most
301 COGs, both mercurials elicited their strongest responses, up- or down-regulated, within
302 the first 10 min of exposure (Figure 3); in most cases, the responses were of similar
303 magnitude. At 30 min, the PMA (green) responses remained nearly the same, up- or
304 down-regulated, but $HgCl_2$ provoked responses (red) generally diminished, often
305 sharply. By 60 min, expression in PMA-exposed cells was barely distinguishable from
306 the unexposed cells in all COG categories, whereas $HgCl_2$ exposed cells had notable
307 differential expression in most COG categories.

308 The four well-defined COG categories with the most DEGs were energy
309 production (C), amino acid metabolism (E), carbohydrate metabolism (G), and
310 transcription (K), which are also categories with a large number of genes (284, 355,
311 381, and 294 respectively) in *E. coli* (Figure 3 legend). COG categories R and S
312 encoding poorly defined (261) or non-defined (203) genes were also represented
313 proportionally. These data suggest both mercurials broadly affect most metabolic
314 categories, albeit to different degrees and at different rates. However, four well-defined
315 COG categories have strikingly different responses to $HgCl_2$ and PMA. COG categories
316 for nucleotide metabolism (F), translation (J), motility (N), and intracellular trafficking (U)
317 have many fewer up-regulated genes in $HgCl_2$ exposed cells than in PMA-exposed
318 cells. There are relatively few DEGs involved in cell division (D), extracellular structures
319 (W), and mobile genetic elements (X) and genes within these categories responded

similarly to both mercurials. Thus, grouping DEGs by COGs illuminates the broad functional differences and similarities between $HgCl_2$ and PMA exposure. Moreover, this view makes clear that DEGs occur in all functional categories for both compounds, but still display distinct differences in global transcriptional response to each compound. We provide gene-level detail on several of these functional groups below. Note that the COG database only includes functional annotations for 3,398 of *E. coli's* 4,497 genes, but functional categories discussed below in more detail are not limited to COG-annotated genes.

A heat map of the DEGs log-fold changes (Figure 4) provides a more granular look at all DEGs for both compounds across all time points. The heat map, using Ward's minimum variance clustering method [36], shows considerable uniformity of up- and down-regulated expression during the 30 min after PMA exposure. In contrast, although $HgCl_2$ exposed cells grossly shared many DEGs with PMA-exposed cells (Figure 2), the heat map reveals a more variegated response to Hg(II) in which different genes are up- or down-regulated at all time points, in contrast to the relatively consistent response of PMA during recovery. Overall, 34% of DEGs are unique to only one mercurial and ~3% of all DEGs had an opposite response to each compound (Table S5). The most dramatic differences were at 60 min when $HgCl_2$ exposed cells were still modulating many genes but PMA-exposed cells had only minor differences with unexposed cells, consistent with their faster recovery of normal growth (Figure 1a). We dissect some of these differences in function-specific heat maps below.

We also used STRING (version 10.0) [37, 38] for unsupervised network analysis to identify gene clusters that were up-regulated in response to each compound (Figure

S8 and Table S7). We focused on up-regulated genes on the working assumption that they are more likely to contribute to recovery than genes whose expression is turned down. Gene clusters were generated by STRING based on organism specific data mining to identify genes with a functional association, such as a common biological purpose, location within the same operon, or shared regulatory mechanism. Note that this network algorithm does not consider fold-change intensity of response; it enumerates only whether an up-regulated gene is present at a given time point. The up-regulated DEGs (nodes) of $HgCl_2$ exposed cells formed several tight clusters encompassing 16 gene-ontology functions (GOFs) at 10 min, nine GOFs at 30 min, and seven GOFs at 60 min (Figure S8 and Table S7). In contrast, although there were more nodes for PMA-exposure at 10 and 30 min, there were fewer edges yielding no well-defined clusters at 10 min and only two GOFs at 30 min. This network analysis suggests that, although PMA provokes more DEGs than Hg(II) does, there is less functional congruence between the genes involved in the response to PMA. Specific gene and function changes are discussed further in the next section.

Lastly, as a control for using RNA-Seq in a longitudinal experiment, we observed DEGs at sequential time points in the unexposed control culture (Figure S9 and Table S8). As expected, changes were gradual over time with no more than 5% of the genome being differentially expressed from one time point to the next. At the 60 min time point, as the cells approached stationary phase 815 genes were differentially expressed compared to mid-log (time 0). Sorting these DEGs by COGs (Figure S9) and by STRING network analysis (Figure S10 and Table S7) showed, as expected, many DEGs were consistent with normal transitioning from mid-log to late-log phase [39, 40].

366

367 ***Higher resolution view of expression differences in specific functional groups***
368 ***during recovery from exposure to $HgCl_2$ or PMA***

369 Taking the perspective that a toxicant is a kind of signaling molecule, we
370 considered differences in gene expression for the two Hg compounds to reflect how the
371 cell senses the biochemically distinct damage produced by these two metallo-
372 electrophiles as manifest by what tools the cell calls upon to restore its viability. A quick
373 snapshot of the great extent of these compound-specific differences can be seen in the
374 genes with a >20-fold increase in differential expression after $HgCl_2$ exposure (Table 1)
375 or PMA exposure (Table 2). Here we emphasize up-regulated genes on the working
376 assumption they could contribute directly or indirectly to repairing damage caused by
377 mercurial exposure. The 25 genes highly up-regulated by $HgCl_2$ (Table 1) are involved
378 in altering the cell surface, oxidative stress response and repair, protein chaperones,
379 metals homeostasis, and ribonucleotide reductase. The vestigial prophage genes likely
380 play no rescue role for the cell and were simply activated by generalized stress
381 responses and have large fold-change values due to repressed expression under
382 normal growth conditions. The corresponding PMA response echoed only 8 of these 25
383 $HgCl_2$ high-responders, and notably did not include the vestigial phage genes.

384 For PMA, the highly up-regulated genes are a distinct contrast to those for $HgCl_2$.
385 First, the maximum amplitude of the PMA-provoked differential expression is generally
386 much less than for Hg(II)-provoked high differential expression (Table 1), which could
387 reflect the lower uptake of PMA. Secondly, while 11 of the 17 PMA-provoked genes

were also on the $HgCl_2$ highly differential expression list, ion transport and antibiotic resistance loci were more prominent with PMA and prophage genes were absent.

These two snapshot tables make the points that both mercurials generate broad, but idiosyncratic, cellular responses. To place these "tips of many icebergs" in their larger cellular context, we used heat maps and tables of subsets of functionally related genes to discuss the differential effects of $HgCl_2$ and PMA on twelve canonical cellular systems in the following sections.

i. INFORMATIONAL MACROMOLECULES

(a) DNA replication, recombination and repair

Of the 24 genes for initiation and maintenance, and termination of chromosome replication, there were more genes down-regulated (8) than up-regulated (3) in response to $HgCl_2$ and an equal number up- or down-regulated genes (7) in response to PMA (Table S9). Of the 14 genes encoding the replicative polymerase holoenzyme, four genes capable of translesion synthesis (*polB*, *dinB*, *umuCD*) were up-regulated more by $HgCl_2$ exposure (Table S9), suggesting a greater degree of direct or indirect DNA damage by $HgCl_2$ exposure. Of the 45 genes for repair and recombination proteins the transcriptional response to each mercurial was very similar (11 up-regulated and 16 down-regulated for $HgCl_2$; 9 up-regulated and 18 down-regulated for PMA). But there were repair genes unique to each compound: *xthA*, *uvrAB*, *mutM,* and *recN* were only up-regulated by $HgCl_2$; and *mutH* and *mutY* were only up-regulated by PMA.

The *recA, recN,* and *xthA* DNA repair genes were ~~the most~~ highly up-regulated (≥10 fold) in response only to $HgCl_2$. The *recA* gene, induced by double-strand DNA

411 breaks, serves multiple roles in DNA repair [41, 42]. Curiously, expression of *recBCD,*
412 which is needed for break repair, either did not change or declined compared to
413 unexposed cells for both mercurials. Expression of several genes involved in repair
414 (*recG*, *nth*, *hsdS*, and *mcrC*) were down-regulated by both compounds, but with larger
415 negative fold-changes for PMA than $HgCl_2$. Thus, the cells responded quickly to both
416 mercurials, but some distinct responses suggest these two compounds directly or
417 indirectly yield different kinds of DNA damage.
418
419 *(b) Transcription*
420 Of the core RNA polymerase (RNAP) genes only PMA-exposure increased
421 expression of a single gene *rpoZ* (ω subunit), but expression decreased in the
422 remaining *rpoABC* core genes (Table S10). $HgCl_2$ exposure did not change expression
423 of any RNAP core genes except for a transient 3-fold drop in *rpoA* at 30 min. Only one
424 of the five termination factors, the Rho-directed anti-terminator, *rof,* increased and did
425 so for both mercurials with PMA again provoking a greater response.
426 Genes for three sigma factors displayed increased expression upon exposure to
427 either mercurial, with *rpoH* (heat shock sigma factor) and *rpoS* (stationary phase and
428 stress response sigma factor) increasing more following PMA-exposure and *rpoD*
429 (housekeeping sigma factor) only increasing after $HgCl_2$ exposure. The effects of $HgCl_2$
430 or PMA exposure on the regulation of genes within each regulon controlled by *E. coli's*
431 seven sigma factors are tabulated in Table S11. Many genes are modulated
432 differentially by $HgCl_2$ or PMA-exposure, but no single sigma factor is uniquely
433 responsible for increases or decreases in responses to these two compounds.

Many of the 203 transcriptional regulators annotated in the RegulonDB (Table 3) [43, 44] and the 1,723 genes they control were expressed differently with the two mercurials (Table S12). PMA provoked up-regulation of more transcription factor genes at 10 and 30 min than $HgCl_2$ exposure, but slightly fewer down-regulated regulators (Table 3). Of all COG categories, transcription had the most up-regulated genes for both mercurials (Figure 3 and Table S6). PMA up-regulated ~40% more transcription related genes at 10 min and ~80% more genes at 30 min than $HgCl_2$. Six activators (*mhpR, glcC, gadX, soxS, mlrA, phoB*) and three repressors (*mcbR, iscR, betI*) were up-regulated at all times for $HgCl_2$, but *gadX* was the only activator gene up-regulated at all times for both mercurials (Table S12). GadX is part of the RpoS regulon [45] and activates the acid resistance system and multidrug efflux [46, 47]. Details of transcription factors and their regulons are provided in Table S12.

Lastly, *E. coli* has 65 currently annotated (ASM584v2), small non-coding RNAs. Although our RNA purification and library preparation methods were not optimized for their enrichment, we observed differential expression for a number of them (Table S5, feature type “ncRNA”). ncRNAs up-regulated for both mercurials are involved in regulation of acid resistance (*gadY*), oxidative stress (*oxyS*), and multiple transporters (*gcvB* and *sgrS*). In contrast, adhesion and motility (*cyaR*), and anaerobic metabolism shift (*fnrS*) were down-regulated by both compounds.

(c) Translation

Upon $HgCl_2$ exposure 83% and 74% of ribosomal proteins (r-proteins) were down-regulated at 10 and 30 min, respectively, versus only 4% and 41% for PMA at the

457 corresponding times (Figures 5 and S9; data for all functional group heat maps are
458 shown in Table S13 and Table S14). Transcription of r-proteins is repressed directly by
459 binding of the nutritional stress-induced nucleotide ppGpp and DksA protein to RNAP
460 [48]. The ppGpp synthase genes, *spoT* and *relA*, were down-regulated or unchanged,
461 but expression of *dksA* was up-regulated for both $HgCl_2$ and PMA exposure. R-protein
462 expression can also be inhibited by excess r-proteins binding to and inhibiting
463 translation of their own mRNAs [49, 50].
464 Translation initiation and elongation factors were largely unchanged, but
465 expression of all three peptide chain release factor genes were down-regulated for PMA
466 and the ribosome recycling factor (*frr*) was up-regulated only for PMA, consistent with
467 interruption of translation. Eight tRNA-synthase genes declined with $HgCl_2$ but PMA
468 caused only four tRNA-synthase genes to decline and two to increase in expression
469 (Table S14). Both mercurials caused a relative decline in tRNA expression for most
470 amino acids, especially arginine, lysine, methionine, tyrosine, and valine tRNAs. With
471 very few exceptions, ribosome assembly and translation were shut down for up to 30
472 min by both compounds, but returned to normal levels by 60 min.
473
474 *(d) Macromolecular turnover and chaperones*
475 Divalent inorganic mercury can stably crosslink proteins and their subdomains
476 via cysteines, disrupting 3-dimensional structures and allosteric movements [51-53].
477 Although monovalent PMA cannot cross-link, it forms a bulky adduct with cysteines [23],
478 which may compromise protein folding. The proteases and chaperones of the heat
479 shock response degrade or repair misfolded proteins [54] and we found their expression

480 was increased by both mercurials (Figures 6 and S12 and Table S13). At 10 min,
481 expression of protease genes *lon, clpXP,* and *ftsH* had risen 4- to 6-fold with $HgCl_2$ and
482 *lon* and *clpXP,* but not *ftsH,* were up-regulated 3-fold with PMA. $HgCl_2$ provoked up-
483 regulation of all 12 heat shock protein (HSP) and chaperone genes by 10 min, but only
484 chaperones *clpB* and *ybbN* mRNAs remained elevated at 30 min. Two other HSP
485 genes, Hsp15 (*hslR*) involved in stalled ribosome recycling and Hsp31 (*hchA*) an amino
486 acid deglycase, were further up-regulated by $HgCl_2$ at 60 min. In contrast, at 10 min
487 PMA had up-regulated only five HSPs, increasing to six by 30 min and declining to three
488 by 60 min. The *ibpA* and *ibpB* chaperone genes were among the most highly up-
489 regulated genes for both $HgCl_2$ and PMA and persisted throughout recovery.
490 Of the 16 RNases and RNA processing enzymes only 3 increased: RNase R (3-
491 fold for $HgCl_2$ and 5-fold for PMA) for both compounds during first 30 min; RNase III
492 two-fold for PMA at 30 min; and RNase T two-fold for $HgCl_2$ at 60 min. The
493 degradasome complex subunit genes (*rne, eno, rhlB, pnp, ppk*) [55] were all down-
494 regulated for PMA during the first 30 min following exposure, except the helicase (*rhlB*),
495 but only enolase was down-regulated for $HgCl_2$ (Figures 6 and S12 and Table S13).
496 Expression of RNase II (*rnb)* was also down-regulated for both compounds, but with
497 relatively greater fold-changes observed for PMA. It is unclear what effect these
498 changes in gene expression could have on RNA turnover and message decay rates
499 while under mercury stress. As with the DNA metabolism genes, expression of the
500 transcriptional apparatus shows that sufficient PMA was taken up to elicit both positive
501 and negative responses distinct from $HgCl_2$.
502

503 ii. ENERGY PRODUCTION

504 *(a) Electron transport chain*

505 Expression of approximately 50% of all electron transport chain (ETC) genes was
506 down-regulated during the first 30 min for $HgCl_2$ and PMA, with individual gene
507 responses being very similar for both compounds (Figures 7 and S13 and Table S13).
508 By 60 min, only 26% of these genes were down-regulated for $HgCl_2$, and none were
509 down-regulated for PMA. Expression of NADH:unbiquinone oxidoreductase genes was
510 down-regulated by both compounds, with 77% and 100% of these genes being down-
511 regulated at 10 and 30 min, respectively. The ATP-synthase subunit genes were also
512 strongly down-regulated by both mercurials at 10 and 30 min, but normal expression
513 was restored at 60 min.

514 The *torCAD* locus that encodes the trimethylamine N-oxide anaerobic respiratory
515 system was strongly up-regulated only by PMA exposure. This is likely an artifact of
516 low-level basal expression and the dimethyl sulfoxide used to dissolve PMA. The final
517 DMSO concentration, 0.015% vol/vol (2.1 mM), was not expected to have any biological
518 effect [56] and the anaerobic DMSO reductase genes (*dmsABC*) were down-regulated.
519 It is unlikely that either the *tor* or *dms* responses affect growth rate [57] or afford
520 protection against either mercurial since over-expressed heme-dependent *torC* may be
521 in the apoprotein form [58].

522

523 *(b) Carbon metabolism*

524 Expression of genes for carbon metabolism decreased generally, but there were
525 more up-regulated genes in response to $HgCl_2$ and not all steps were affected equally

526 by both mercurials (Figure S14). Expression of five genes of the pentose-phosphate
527 pathway rose in at least one time point for $HgCl_2$, but only *pgl* increased for PMA at 10
528 min. The ribose-5-phosphate isomerase gene (*rpiB*), which is a backup enzyme for the
529 gene product of *rpiA* [59], was up-regulated 40-fold for $HgCl_2$ at 10 min; although
530 expression of *rpiA* did not differ from the unexposed cells for either mercurial at any
531 time. Glycolysis responded similarly to both mercurials, with the greatest number of
532 these genes being down-regulated at 30 min. The expression changes in TCA cycle
533 genes were distinct for $HgCl_2$ and PMA; six genes were up-regulated in at least one
534 time point for $HgCl_2$ and only one was up-regulated for PMA. Expression of several
535 carbohydrate transport genes was down-regulated by both mercurials (Table S6).
536
537 *(c) Nicotinamide adenine dinucleotide (NAD)*
538 Expression of genes for nicotinamide adenine dinucleotide (NAD) and NAD-
539 phosphate (NADP) synthesis and turnover pathways was repressed by mercury
540 exposure (Figure S15). The biosynthesis genes were moderately down-regulated, with
541 *nadB* being the only gene down-regulated for both mercurials at all times and *nadA*
542 decreasing for $HgCl_2$ at 30 and 60 min and for PMA at 30 min. Expression of the
543 *pncABC* salvage pathway did not change. The NAD reduction pathways were more
544 affected than the NADP reduction pathways, with only *pgi* down-regulated for both
545 mercurials and *edd* down-regulated only for $HgCl_2$. The transhydrogenase (*pntAB*) was
546 down-regulated only for PMA at 10 and 30 min. Expression of other genes for NAD to
547 NADH reduction in glycolysis and the TCA cycle were also down-regulated for both

548 mercurials, which reflects the overall decrease in metabolism and energy production
549 pathways.

550 Globally, redox metabolism declined immediately after exposure and normal
551 gene expression levels were not restored until growth recovered to the pre-exposure
552 rate. KEGG maps created using iPath [60] depict system-wide metabolism changes
553 over time (Figures S16-S18 for $HgCl_2$ and Figures S19-S21 for PMA).

554

555 iii. CENTRAL METABOLISM

556 *(a) Amino acid metabolism and transport*

557 The two mercurials had distinct effects on expression of genes for biosynthesis of
558 amino acids (Figure 8 and S22). Since mercury targets cysteine thiol groups and will
559 deplete the cellular reduced thiol pool, we expected an increase in cysteine and
560 glutathione biosynthesis. Surprisingly, most genes for biosynthesis of these biothiols
561 and for general sulfur metabolism were down-regulated or no different from the
562 unexposed cells, with the exception of up-regulation of *cysE*, which is the first step in
563 the biosynthesis pathway from serine.

564 Methionine biosynthesis gene expression increased for 7 genes with $HgCl_2$, but
565 11 genes were down-regulated with PMA, especially *metE* dropping 187-fold with PMA
566 at 30 min (Figure 8 and S22). Expression of genes for histidine synthesis also
567 responded differently to each mercurial, rising dramatically with $HgCl_2$ at 30 to 60 min.
568 In contrast, all *his* genes expression dropped with PMA from 10 to 30 min. Genes for
569 the synthesis of leucine, isoleucine, and valine had the opposite response, with most
570 down-regulated with $HgCl_2$ but up-regulated with PMA. Expression of other amino acid

biosynthetic pathways was largely unchanged or declined with both mercurials. Branched-chain (*livKHMGF*), dipeptide (*dppABCDF*), and oligopeptide (*oppABCDF*) transporters were also down-regulated for both mercurials, with greater relative negative fold-changes for PMA (Table S5).

(b) Inorganic ion transport and metallochaperones

Inorganic Hg(II) can displace beneficial thiophilic metals from their native binding sites in proteins, potentially affecting transport and disrupting transition metal homeostasis [23], leading to expression changes for non-ferrous metal cation and oxoanion transporters (Figures 9 and S23 and Table S13), iron homeostasis (Figures 10 and S24 and Table S13) and metal-binding proteins and enzymes (Table S15).

Inorganic mercury exposure releases labile iron, which could itself increase oxidative stress via Fenton chemistry under aerobic growth [23, 61]. Most iron uptake pathways declined early for both mercurials, consistent with the observed increase in expression of the Fur repressor. The cytochrome *c* maturation genes that transport heme to the periplasm (*ccmABCDE*) were also down-regulated for both mercurials. The putative ferrous iron and zinc efflux pump, *fieF* [62] increased 2-fold for $HgCl_2$ at 10 min only, suggesting it may have a transient role in restoring one or both of these homeostases.

There are two iron-sulfur (Fe-S) cluster assembly pathways in *E. coli* [63, 64]. Expression of the primary Isc system (*iscRSUA*, *hscBA*, and *fdx*) increased strongly for both mercurials, but with greater relative changes for $HgCl_2$ (Figures 10 and S24 and Table S13). The secondary Fe-S cluster assembly system *sufABCDSE*, which activates

under oxidative stress or iron limiting conditions also increased greatly, but only for $HgCl_2$. These transcriptional responses confirm and extend biochemical findings [23] that Fe-S clusters are more vulnerable to inorganic mercury than to organomercurials and the cell quickly tries to repair this damage.

Expression of the zinc transporter *zupT* increased modestly in the 3- to 5-fold range for both mercurials during the first 30 minutes (Figures 9 and S23 and Table S13). In contrast, expression of the P-type ATPase zinc efflux pump, *zntA* [65] increased in the 20- to 40-fold range for both mercurials at 10 and 30 min and the periplasmic Zn-binding protein ZraP was up-regulated throughout recovery. *E. coli* has two copper/silver efflux systems, Cue and Cus [66]. Surprisingly, the Cus system genes (*cusRS, cusCFBA)* primarily used under anaerobic conditions were among the most down-regulated genes under PMA exposure. The Cue system consists of the multi-copper oxidase, CueO, and a P-type ATPase, CopA, both regulated by the MerR homolog, CueR. Genes *cueO* and *copA* were up-regulated approximately 20-fold with $HgCl_2$ at both 10 and 30 min whereas they increased 5-fold with PMA only at 10 min. The nickel uptake system [67] (*nikABCDER*) was also strongly down-regulated under PMA exposure conditions through all times although expression of repressor NikR was unchanged, except for a 3-fold increase with $HgCl_2$ at 10 min. Expression of the nickel and cobalt efflux gene, *rcnA*, increased with $HgCl_2$ or PMA. Manganese (*mntH*), and magnesium (*mgtA, corA*) uptake genes increased with both mercurials.

Inorganic anions used by *E. coli* include phosphate, sulfate, and molybdate and the genome also encodes genes for defense against arsenate, which acts as a phosphate mimic (Figures 9 and S23 and Table S13). Expression of the ABC

phosphate transport system (*pstSCAB*) genes increased greatly for both mercurials, with PMA-provoked changes up to 165-fold, relative to unexposed condition, for the phosphate binding protein, *pstS*. The two-component phosphate regulatory system, PhoBR, was up-regulated for both mercurials; *phoB* changed up to 22-fold with $HgCl_2$ and 105-fold with PMA relative to the unexposed condition. Sulfate and thiosulfate uptake by the ABC transporter (*cysPUWA*) decreased strongly with $HgCl_2$ at 30 min and PMA at 10 and 30 min. Expression of molybdate uptake (*modABC*) increased with PMA during the first 30 min but only at 10 min with $HgCl_2$. The arsenate resistance operon cannot effect Hg(II) resistance, but was highly induced by both mercurials, perhaps through interacting with the three-cysteine metal-binding site of the ArsR repressor [68].

iv. SURFACE FUNCTIONS

(a) Cell wall biogenesis, porins, lps, efflux systems, and electrolyte balance

The transcriptional response of peptidoglycan, membrane biosynthesis, and cell division genes was similar for both mercurials (Figure S25 and Table S13). Expression increased for roughly 20% of lipid biosynthesis genes, including those for cardiolipin, and expression decreased for 20-30% of other lipid-related genes. Transcription of genes for murein synthesis (*murCDEFGIJ*) in particular declined for both mercurials during the first 30 min.

E. coli encodes several antibiotic resistance efflux systems that are up-regulated by mercury exposure (Figures 11 and S26 and Table S13). The multiple antibiotic resistance locus (*marRAB*), which increases drug efflux and also limits passive uptake by decreasing porin expression [69], was strongly up-regulated by both mercurials with

640 greater fold-changes observed for PMA, relative to the unexposed condition. Though
641 expression of some porin genes (*ompC, ompF, ompT, ompW*) was repressed, three
642 non-specific porins (*ompG, ompL, ompN*) were up-regulated only by PMA. Genes from
643 several TolC-dependent antibiotic efflux systems were up-regulated by both mercurials
644 as well, including *acrEF, emrD, emrKY,* and several *mdt* genes [70]. $HgCl_2$ exposure
645 alone also up-regulated two-component sensor genes (*phoQP* at 10 min and *basSR* at
646 60 min) that regulate genes involved in modification of the cell surface and increase
647 polymyxin resistance [71], but most of these genes were down-regulated or unchanged
648 for PMA.

649 The response to osmotic stress and maintenance of electrolyte balance are
650 important membrane functions requiring adaptation in dynamic natural environments.
651 During $HgCl_2$ exposure the expression of the sodium antiporter, NhaA, increased 4-fold
652 at 10 min and the calcium/potassium antiporter, ChaA, was up-regulated 3-fold at 10
653 and 30 min (Figures 9 and S23 and Table S13). In contrast, expression of genes for
654 transport of the major electrolyte, potassium, changed only modestly in some subunits
655 of the *kdp, kef*, and *trk* systems, without an obvious response pattern. However,
656 transcription of genes for defense against osmotic stress was uniformly up-regulated;
657 betaine genes (*betABIT and proP*), *osmBCEFY, and* mechanosensitive channel
658 proteins (*mscL* and *mscS*) increased for both mercurials, as did a putative
659 osmoprotectant ABC permease (yehYXW) [72] only with $HgCl_2$ at 30 and 60 min (Table
660 S5).

661

662 *(b) Motility and biofilm*

663 Nearly all flagellar component genes were strongly down-regulated for both
664 mercurials, with greater negative fold-changes observed with PMA relative to the
665 unexposed condition (Figures 12 and S27). Only PMA increased expression of fimbriae
666 and curli fiber genes, which alter motility and increase adhesion (Figure 13 and S28)
667 [73]. Fifteen genes up-regulated by PMA exposure were annotated as homologs of
668 FimA, but with unknown function. FimA is the major structural component of fimbriae,
669 but these genes may serve other functions. Motility genes whose expression dropped
670 remained low until 60 min with $HgCl_2$, indicating that the structurally and energetically
671 intensive motility systems are very slow to recover.
672 $HgCl_2$ and PMA also provoked expression of several biofilm-related genes
673 (Figures 13 and S28 and Table S13). The *bhsA* and *bdcA* loci were among the most
674 highly up-regulated genes during $HgCl_2$ exposure, with a relatively greater fold-change
675 than observed for PMA (Tables 2 and 3). Neither gene is well characterized, but
676 independently each has been found to decrease biofilm formation and increase
677 resistance to external stressors [74, 75]. Only PMA increased expression of genes for
678 poly-β-1,6-N-acetyl-glucosamine (PGA) polysaccharide production [76] and biofilm
679 related genes, *ycgZ, ymgA, ariA, ymgC* [77]. Thus, PMA elicits a broader response that
680 potentially alters the cell surface and may increase adhesion and biofilm formation; in
681 contrast $HgCl_2$ only inhibits motility and does not activate adhesion pathways. It is
682 possible that some changes observed for motility and biofilm related genes following
683 PMA-exposure are an artifact of the DMSO, but other studies suggest that solvent
684 would have no effect or that much higher concentrations than used here would be
685 required to induce these changes [56, 78].

686

687 v. STRESS RESPONSES

688 *(a) Oxidative stress response and repair*

689 There are two oxidative stress response pathways in *E. coli*, the *oxyRS* and
690 *soxRS* regulons [61, 79]. OxyR, a LysR-family transcriptional regulator, uses a cysteine-
691 pair to sense oxidative damage and regulates 49 genes when oxidized [80]. $HgCl_2$
692 exposure increased expression of 22 OxyR regulon genes at 10 min; these then
693 declined to 13 genes by 60 min (Table S16). In contrast, PMA provoked expression of
694 16 OxyR regulon genes at 10 and 30 min, but none at 60 min. *OxyS*, a small non-
695 coding RNA regulated by OxyR, represses *rpoS*, *fhlACD* and other genes to prevent
696 redundant induction of stress response genes [81]. The *oxyS* gene was among the most
697 highly differentially expressed genes, increasing over 1,000-fold with $HgCl_2$ at 10 and 30
698 min relative to the unexposed condition. Differential expression of *oxyS* was more
699 modest with PMA having a relative increase of 10-fold at 10 min and 6-fold at 30 min.
700 The SoxRS regulon is the other oxidative stress response system in *E. coli*.
701 SoxR, a MerR-family repressor-activator, uses the oxidation state of 2Fe-2S clusters to
702 respond to superoxide (O_2^-) stress and induce transcription of *SoxS* [82-85], which then
703 transcriptionally regulates 53 genes [79, 86] (Table S16). $HgCl_2$ or PMA exposure up-
704 regulated 22 or 25 genes, respectively, at 10 min and these had declined to 13 or 0
705 genes, respectively by 60 min.
706 Key genes in these oxidative stress regulons differentially expressed upon
707 mercury exposure include the ROS scavengers: catalase (*katG*), alkyl hydroperoxide
708 reductase (*ahpCF*), and superoxide dismutase (*sodA*) (Figures 14 and S29 and Table

709 S13). Thiol homeostasis genes included *gor*, *grxA,* and *trxC* (Figures 14 and S29 and
710 Table S13). Iron homeostasis and the Fe-S cluster assembly and repair genes (*fur, dps,*
711 *fldA, fpr, hemH, sufABCDES,* and *yggX*) were also up-regulated. PMA provoked
712 comparatively lower fold-changes than $HgCl_2$ for *grxA, trxC, ahpC, dps, fldA, hemH, and*
713 *yggx*. The manganese uptake protein, *mntH*, plays an important role in ROS resistance
714 [87] and was up-regulated for both mercurials. Oxidation-resistant dehydratase
715 isozymes, *acnA* and *fumC* [88, 89] also increased, but only for $HgCl_2$ exposure. Thus,
716 both mercurials triggered the Oxy and Sox oxidative stress responses, but $HgCl_2$
717 elicited greater fold-changes overall than PMA compared to unexposed cells.
718 Because mercury poisons the cellular thiol pool [23], we expected that regulation
719 of redox homeostasis proteins such as glutaredoxins, thioredoxins and glutathione-
720 related genes would respond to mercury exposure (Figure 14 and S29). Glutaredoxin 1
721 (*grxA*) expression was up-regulated for both mercurials, with a greater fold-change
722 observed for $HgCl_2$ relative to unexposed condition. In contrast, glutaredoxin 2 (*grxB*)
723 was down-regulated for both mercurials, while glutaredoxin 3 (*grxC*) and glutaredoxin 4
724 (*grxD*) were up-regulated only for PMA. Thioredoxin reductase (*trxB*) was up-regulated
725 2-fold with PMA only at 30 min, but was up-regulated with $HgCl_2$ 8-fold (10 min) and 4-
726 fold (30 min). Thioredoxin 1 (*trxA*) expression increased 2-fold only with PMA (10 min);
727 in contrast to thioredoxin 2 (*trxC*), which was up-regulated for both mercurials, but had
728 greater fold-change relative to the unexposed condition with $HgCl_2$ than with PMA.
729 However, the thiol peroxidase (*tpx*) was up-regulated modestly for PMA, but did not
730 change for $HgCl_2$. Thus, while each mercurial stresses the cell to maintain redox
731 homeostasis, $HgCl_2$ exposure elicited greater responses.

Glutathione (GSH) serves as the cell's redox buffer and as a scavenger of mercurials (Figures 14 and S29 and Table S13). Surprisingly, expression of GSH biosynthesis and utilization genes increased only modestly. The γ-glutamyltranspeptidase (*ggt*) increased late (60 min) by 4-fold only with $HgCl_2$. GSH synthase (*gshA*) did not change and *gshB* was up-regulated 2- or 3-fold for both mercurials only at 10 min. The GSH importer (*gsiABCD*) may be a salvage pathway to recover GSH and cysteine leaked into the periplasm by CydCD [90, 91], but it was down-regulated by $HgCl_2$ or PMA through 30 min. The GSH reductase (*gor*) increased only with $HgCl_2$ at 10 min and several GSH S-transferase genes involved in detoxification [92] (*gstA, gstB, yfcF, yqjG, yibF, yncG*) increased with both mercurials. Since all of these proteins have Hg(II)-vulnerable cysteines in their active sites, it is surprising that neither Hg(II) nor PMA-challenged cells provoked increased expression and suggests that their normal mRNA levels are sufficient to replenish them.

(b) Genes with delayed up-regulation

Genes unchanged at 10 min but differentially expressed at both 30 and 60 min or 60 min alone may be those needed as cells transition out of stasis and towards normal growth (Table S17). For $HgCl_2$ exposure, 95 genes were up-regulated and 140 genes were down-regulated that display this delayed response pattern. Approximately half of the up-regulated genes are involved in energy production, transport and metabolism pathways based on COG annotations. Roughly 45% of these delayed $HgCl_2$ provoked, up-regulated genes are the same as genes that were differentially expressed during the first 30 min of PMA exposure. This overlap is consistent with slower recovery of growth

in $HgCl_2$ exposed cells and that some of the same pathways are used for recovery by both compounds. In contrast, for the more quickly recovering PMA exposure, of the genes that showed no change at 10 min only six were up-regulated at 60 min (Table S17). Only two of these delayed-response genes for PMA exposure overlapped with up-regulated genes for $HgCl_2$ exposure.

DISCUSSION

Mercury is a ubiquitous toxicant that serves no biologically beneficial role. Exposure to any form of mercury negatively impacts the health of organisms from microbes to humans. The biological effects of different forms of mercury are often conflated and methylmercury is assumed to be the most toxic form. However, the systemic biochemical and molecular differences between inorganic and organic mercury compounds have yet to be well characterized from exposure through recovery in a single model system.

BULK DIFFERENTIAL EFFECTS ON GROWTH AND GENE EXPRESSION

The sub-acute mercury exposure conditions used in this study were chosen by identifying a mercury concentration high enough to stop cells from doubling, but low enough to allow restoration of the pre-exposure growth rate within one-hour (~1 generation period) after exposure (Figure 1a). Concentrations below 3 μM of either compound did not consistently inhibit growth and higher concentrations of $HgCl_2$ did not allow recovery within the desired time frame. The 3 μM Hg used in this study is well within the range that bacteria can experience chronically from dental amalgam fillings

778 [93] and in highly contaminated environments, such as artisanal gold mining operations
779 [8]. Mercury in tuna is 0.386 ppm compared to the proxy organomercurial, PMA, used
780 here at 3 μM or 0.6 ppm [94].

781 PMA-exposed cells recovered exponential growth faster (Figure 1) than those
782 with equimolar exposure to $HgCl_2$, perhaps owing to lower uptake of PMA (Table S2).
783 However, PMA-exposed cells differentially expressed more genes than $HgCl_2$ exposed
784 cells during the first 30 min of exposure (Figure 1b). These results agree with
785 observations in *C. elegans,* where MeHg exposure resulted in four times more DEGs
786 than did $HgCl_2$ for all concentrations tested [95]. However, in contrast to *E. coli,* whose
787 growth was inhibited more by inorganic $HgCl_2$, in *C. elegans* the effective toxic
788 concentration of methylmercuric chloride was lower than for $HgCl_2$ [95]. The large
789 number of significant DEGs in response to mercury exposure is greater than the
790 response to hydrogen-peroxide [96] or nitric-oxide [97], but other types of chemical
791 exposures to organic acids [98] and volatile organic compounds [99] in *E. coli* have
792 resulted in similar numbers of DEGs to mercury exposure and the stress response
793 sigma factor RpoS has been shown to regulate up to 23% of the genome alone [100].

794 We found that most DEGs peaked at 10 min after exposure for both compounds
795 with $HgCl_2$ provoking more down-regulated genes and PMA yielding more up-regulated
796 genes throughout the exposure period (Figure 1b). Even though the optical density (OD)
797 of the $HgCl_2$ exposed culture showed no growth recovery from 10 min to 30 min, DEGs
798 decreased by 22%, while PMA-exposed cells over the same period had a moderate
799 increase in OD, but only an 8% decrease in DEGs (Figure 1). In contrast in a eukaryotic
800 system, the livers of $HgCl_2$ exposed zebrafish continuously increased in DEGs

801 throughout the observed 96 hour exposure period as mercury accumulated in their cells
802 [101].

803 In *E. coli,* during the first 30 min post-exposure, 50-70% of both up- and down-
804 regulated genes were the same for both compounds (Figure 2), but at the level of
805 individual genes there were both qualitative and quantitative differences in expression
806 (Table S5), consistent with idiosyncratic transcriptional responses to each compound.
807 The nematode *C. elegans* also manifested distinct and even some opposite
808 transcriptional responses to inorganic and organic mercury exposure in a single end-
809 point microarray experiment [24].

810 As there are not yet other studies of the global transcriptional response of a
811 bacterium to mercury exposure, on the basis of the findings in eukaryotes and our
812 proteomic work [23] we have organized our observations here into those we had
813 expected and those we did not expect from any yet published work.

814

815 ***EXPECTED AND UNEXPECTED GENE-SPECIFIC CHANGES***

816 *Expected transcriptional changes:*

817 *(a)* Thiol homeostasis. The millimolar cytosolic pool of glutathione (GSH) can sequester
818 mercurials and thereby protect protein thiols from binding strongly to these soft metal
819 toxicants. However, if the GSH pool becomes depleted by mercury complexation, the
820 cell loses this primary defense mechanism. Since proteins of the stress response and
821 repair pathways all contain active site thiols, often as part of Hg(II)-vulnerable Fe-S
822 centers, it is not obvious how a cell that has lost much of its available thiols to Hg(II)
823 chelation can restore its metabolism. Given this, we expected cysteine and glutathione

biosynthesis pathways to be up-regulated. However, cysteine biosynthesis was down-regulated (Figures 8 and S22 and Table S13) and GSH biosynthesis was mostly unchanged (Figures 14 and S29 and Table S13) for both compounds, in contrast to the eukaryotic response to mercury [101-103] and H_2O_2 exposure [96], which increase GSH and metallothionein production. However, although thiol biosynthesis did not increase, genes involved in maintaining cellular thiol homeostasis did increase (Figures 14 and S29 and Table S13); thioredoxin (*trxC*) and glutaredoxin (*grxA*) were among the most highly up-regulated genes with $HgCl_2$ and PMA exposure. Others have also found in *E. coli* that glutathione reductase increased with $HgCl_2$ and both compounds increased expression of glutathione oxidoreductase and S-transferase genes, which protect against oxidative stress and xenobiotics [104].

(b) Iron homeostasis. We also expected inorganic mercury to disrupt iron-sulfur clusters with consequent effects on Fe homeostasis generally [23, 105]. Iron uptake was down-regulated with both mercurials, consistent with excess intracellular free Fe(II) and general oxidative stress, but expression of the uptake repressor (*fur*) was only up-regulated for $HgCl_2$ (Figure 10 and S24). *Fur* expression is activated by either OxyR or SoxS [96, 106] and Fur represses Fe uptake pathways with ferrous iron as a co-repressor [107]. Fur can also bind other divalent metals [108], so Hg(II)-Fur might mimic Fe-Fur as an iron uptake repressor under these conditions to limit Fenton-mediated damage from excess iron. Although both mercurials increased expression of the primary Fe-S cluster assembly and repair system (*isc*), only $HgCl_2$ induced the secondary system (*suf*), which is normally induced under oxidative stress or iron limiting conditions

847 [63, 109] (Figures 10 and S24 and Table S13). Also, only $HgCl_2$ exposure increased
848 expression of iron storage proteins: ferritin, bacterioferritin, and Dps (Figure 10 and
849 S24). The DNA binding protein Dps which binds free iron to protect DNA from ROS
850 damage [110] was one of the most highly up-regulated genes with $HgCl_2$ exposure
851 (Table 1).
852
853 *(c)* Oxidative stress response. The known close link between iron homeostasis and
854 oxidative stress [61] explains the large fold-changes observed upon $HgCl_2$ exposure in
855 genes that respond to oxidative stress (Table S16) and echoes mercury's long known
856 stimulation of oxidative damage in rat kidney mitochondria [111]. The small non-coding
857 RNA *oxyS* was the second most highly up-regulated gene upon $HgCl_2$ exposure with
858 differential expression more than 100-fold greater than observed for PMA (Table 1). The
859 ROS scavenger *ahpF* was also highly up-regulated, along with *katG* (early) and *sodA*
860 (delayed) but only for $HgCl_2$ (Figures 14 and S29 and Table S16). Other ROS resistant
861 enzymes, aconitase A [89] and fumarase C [112] (Table S16) also increased only for
862 $HgCl_2$, as did the manganese-dependent alternative ribonucleotide reductase genes
863 (*nrdHIEF*) [113]. The glutaredoxin-like protein that functions like thioredoxin, *nrdH* [114],
864 was highly up-regulated by $HgCl_2$ and might support other thioredoxin and glutaredoxin
865 proteins. These striking differences in gene expression illuminate how *E. coli* modulates
866 expression of specific genes not only to deal with compromised function of specific
867 $HgCl_2$ modified proteins, but also to manage the consequent cascade of reactive oxygen
868 species.
869

(d) Heat shock response. Mercurials bound to protein cysteines could disrupt protein folding, subunit assembly, and allosteric movements [52, 115] and inorganic mercury can crosslink neighboring cysteines leading to aggregation [51]. Increased expression of heat shock response genes was expected as a consequence of such anticipated protein misfolding problems [116]. Indeed, expression of heat shock chaperonins and protease genes increased for both mercurials, with more genes up-regulated early in response to $HgCl_2$ than to PMA (Figures 6 and S12 and Table S13). Genes for the small chaperone-like proteins, *ibpA* and *ibpB*, were among the most highly increased for both compounds, especially for $HgCl_2$ (Table 1), consistent with their role in aiding Lon protease in the degradation of misfolded proteins [117-119].

(e) Translational apparatus. Thiophilic Cd^{2+} exposure in *E. coli* has been shown to decrease expression of ribosomal proteins [120]. In our proteomics work (Zink et al. in preparation) we observed fourteen r-proteins (7 for each ribosomal subunit) that formed stable adducts with either PMA or Hg(II), so it was reasonable to expect this to be reflected in transcription of r-proteins. Indeed, $HgCl_2$ exposure repressed expression of up to 83% of r-protein genes at 10 min and 74% at 30 min (Figure 5, S11, and Table S14), whereas PMA only transiently repressed expression of 41% of r-proteins at 30 min. Divalent inorganic mercury's ability to cross-link proteins may interfere with ribosome assembly resulting in translational feedback and repression of r-proteins transcription. Disruption of ribosome assembly could also contribute to the slower recovery of growth after inorganic Hg(II) exposure.

893 *(f)* Energy production. The dependence of most energy production pathways on redox-
894 active transition metals and redox-active sulfur compounds made them obvious targets
895 of mercurial disruption, e.g. three ATP-synthase subunits form stable adducts after in
896 vivo exposure to Hg(II) or PMA (Zink et al. in preparation). Expression of genes within
897 this functional category was largely down-regulated early in exposure, with all nine
898 ATPase subunits down-regulated for $HgCl_2$ (10 min) and eight down-regulated for PMA
899 (30 min) (Figure 7 and S13). Although others have found that Cd exposure in *E. coli*
900 repressed aerobic energy metabolism genes and induced anaerobic pathways [120], we
901 found that both aerobic and anaerobic energy metabolism were repressed by $HgCl_2$ and
902 PMA. Even though expression of the oxygen-sensing *fnr* [121] and *aer* [122, 123]
903 activators of the anaerobic shift were moderately up-regulated for PMA and unchanged
904 for $HgCl_2$ (Table S5). Similarly, glucose metabolism genes were also predominantly
905 down-regulated during early periods for both compounds, especially with PMA exposure
906 (Figure S14). Thus, with severely compromised energy production systems, it is not
907 surprising that amino acid, carbohydrate and nucleotide metabolism genes, and the
908 energy-dependent transport of these molecules (Figure 3 and Table S6), are also
909 largely depressed initially.
910
911 *(g)* Homeostases of non-ferrous metals. We expected mercurials to disrupt electrolyte
912 balance [23], but expression of the potassium efflux pumps' subunit genes (*kcpABC,*
913 *kefBC, and trkAGH*) were not uniformly up-regulated, although the need to restore the
914 pH balance was indicated by transiently increased expression of the H^+/Na^+ antiporter
915 (*nhaA*) for both compounds (Figures 9, S23 and Table S5). It may be that normal levels

916 of the proteins involved in maintaining cellular electrolyte balance are sufficient to
917 respond to mercury exposure and a significant change in transcriptional expression is
918 not required for these genes.

919 Mercury is also expected to disrupt non-ferrous metal homeostasis because it
920 can displace other metals, such as zinc and copper, as enzyme cofactors [124, 125].
921 Expression of metal uptake genes decreased and of metal efflux genes increased for
922 zinc, copper, nickel and cobalt, with relatively greater fold-changes occurring with $HgCl_2$.
923 Zinc efflux by ZntA is regulated by the MerR homolog ZntR, which can respond to Hg(II)
924 [126], but has not been shown to confer resistance to Hg(II) exposure. Up-regulated
925 periplasmic transition metal binding proteins, ZraP [127] and ZinT [128], use histidine
926 residues to coordinate metal binding and all cysteine residues present in either protein
927 are involved in structural disulfide bonds that prohibit availability for binding metals.
928 Thus, these periplasmic metal binding proteins lack requisite thiol ligands [23] to
929 compete for Hg effectively with periplasmic glutathione [90, 129, 130]. Their increased
930 transcription here likely reflects their control by a complex suite of redox and other
931 stress regulators [86] provoked by Hg exposure as reported above. Manganese may
932 protect iron metalloenzymes under oxidative stress conditions [87] and Mn uptake by
933 *mntH,* as part of the OxyR regulon, was correspondingly up-regulated for both
934 compounds in response to mercury-induced oxidative stress.
935
936 *Unexpected transcriptional changes:*
937 *(a)* Motility and chemotaxis. Energetically costly flagellar motility and chemotaxis were
938 strongly down-regulated by both mercurials and were among the slowest to recover

939 normal transcription levels (Figures 12 and S27 and Table S13). Motility gene
940 expression is regulated by σ^{28} (*fliA*) and FlhDC [131] and the expression of these two
941 regulatory genes declined with $HgCl_2$ but was unchanged with PMA. Repression of
942 motility may occur through sigma factor competition for binding to RNAP between σ^{28}
943 and increased expression of σ^{S} [132] and/or through repression of the flagellar
944 transcriptional activator FlhDC by increased expression of the small ncRNAs *oxyS* and
945 *gadY* [133]. Interestingly, $HgCl_2$ exposure impaired locomotion in *C. elegans* [24],
946 although through a very different mechanism of motility from *E. coli*.
947
948 *(b)* Surface appendages and biofilm synthesis. Surprisingly, there were large increases
949 in expression of genes involved in biofilm formation and adhesion or dispersal (Figures
950 13 and S28 and Tables S13). Expression of *bhsA* and *bdcA,* which function in biofilm
951 dispersal or reduced biofilm formation [74, 75]*,* were the first and third, respectively,
952 most up-regulated genes by $HgCl_2$ (Table 1) and were also up-regulated for PMA, but
953 with relatively smaller fold-changes (Table 2). Expression of *bhsA* is also up-regulated
954 by other diverse stressors and may decrease cell permeability [75, 134]. PMA exposure
955 especially increased expression of genes for the polysaccharide PGA, which aids in
956 adhesion in biofilm formation [76], and other biofilm formation (*ycgZ, ymgA, ariA, ymgC*
957) genes [77] (Figures 13 and S28 and Table S13).
958 Expression of fimbriae (*fim)* and curli fibers (*csg*), important for adhesion in
959 biofilm formation [73] were also up-regulated only by PMA (Figure 13 and S28), as were
960 15 of 22 FimA homologs of unknown function. Outer membrane vesicle formation
961 (OMVs) could also play a role in detoxification, since an increase in formation of these

962 vesicles has been associated with heat shock, oxidative stress response, and biofilm
963 formation [135], which are responses up-regulated to varying degrees by both
964 mercurials. These are distinct differences between PMA and $HgCl_2$ response. PMA
965 provocation of biofilm formation and adhesion genes might be an artifact of its DMSO
966 solvent, but it is not obvious why $HgCl_2$ induces such high increases in biofilm dispersal
967 genes.
968
969 *(c)* Phosphate metabolism. Phosphate uptake genes were among the most highly up-
970 regulated genes for PMA exposure (Figure 9, S23, and Table 2). The PhoBR two-
971 component system controls expression of phosphate transport genes, as well as some
972 genes that increase virulence including those for fimbriae and biofilm formation [136].
973 Since expression of PhoBR and its regulon increases under phosphate limiting
974 conditions [137], it may be that PMA inhibits phosphate uptake by an unknown
975 mechanism, possibly through direct interaction with highly up-regulated PstS or this
976 could be an artifact of DMSO.
977
978 *(d)* Amino acid biosynthesis. Expression of most amino acid pathways was down-
979 regulated by both compounds, but a few responded uniquely to each mercurial (Figures
980 8 and S22 and Table S13). Since methionine auxotrophy occurs under oxidative stress
981 due to ROS susceptibility of methionine synthase (MetE) [138], expression of
982 methionine biosynthesis genes may have increased with $HgCl_2$ due to a stronger
983 oxidative stress response than PMA. However, since PMA did up-regulate some
984 oxidative stress-related genes, it is curious that Met operon expression was down-

regulated under PMA exposure. Next to its affinity for cysteine sulfur, Hg(II) binds the imino nitrogen of histidine very strongly [139], so it was intriguing that histidine biosynthesis genes were also up-regulated by $HgCl_2$ but down-regulated by PMA. It remains unclear how these differences or the opposite responses for leucine, isoleucine and valine biosynthesis help the cell survive mercurial exposure.

(e) Miscellaneous genes. Multiple antibiotic efflux systems and polymyxin resistance surface modifications were up-regulated by $HgCl_2$ exposure, and even more so by PMA (Figures 11 and S26 and Table S13). Chronic mercury exposure contributes to the spread of multiple antibiotic resistant bacteria through co-selection of plasmid-borne antibiotic and mercury resistance genes [140, 141]. Increased expression of antibiotic resistance and surface components hint that low-level mercury exposure could prime cells for increased antibiotic resistance. However, the ubiquity of plasmid- and transposon-borne Hg resistance loci suggests that expression of these chromosomal genes offers insufficient protection against the antibiotic or mercurial levels encountered in clinical practice.

A handful of vestigial e14 or CPS-53 prophage genes were up-regulated by $HgCl_2$ (Table 1) or PMA (Table S5), respectively. Some are known to increase resistance to osmotic, oxidative, and acid stressors [142, 143], but their roles and mechanisms have not been well defined.

(f) Differential expression of genes required for the same functional protein complex.

In many instances we observed that transcripts for subunits of the same enzyme, protein complex, or component of a tightly articulated pathway were differentially expressed. In some cases these proteins lie in distinct transcripts, which may experience different turnover rates and in other cases the differences could be due to transcriptional polarity. We have chosen not to deal explicitly with such paradoxes in this work, which is sufficiently complex as it is, but will address them in future work.

CONCLUSIONS

The effects of mercury exposure in multicellular organisms have long been studied at the physiological level but a global, fine grained understanding of the differences in the precise biochemical sequelae of inorganic and organic mercury exposure has been lacking. This study is the first to examine not only the global transcriptional response differences between inorganic mercury ($HgCl_2$) and an organomercurial (phenylmercuric acetate) in a model microorganism, but also first to examine longitudinally how the cell recovers from these chemically distinct compounds. Taken together with global identification of vulnerable protein targets (Zink et al. in preparation) and of damage to thiol and metal ion homeostasis upon acute mercurial exposure [23], the current work provides a quantitative systems-level description of the effects of *in vivo* mercury exposure in *E. coli*. What was striking and most challenging with this study was the breadth and diversity of the systems whose expression was affected by these two chemically distinct mercurials. Sub-acute exposure influenced expression of ~45% of all genes with many distinct responses for each compound, reflecting differential biochemical damage by each mercurial and the corresponding

resources available for repair. Energy production, intermediary metabolism and most uptake pathways were initially down-regulated by both mercurials, but nearly all stress response systems were up-regulated early by at least one compound. These results echo the wide functional variety of proteins stably modified by these mercurials owing to the widespread occurrence of cysteines found in nearly all *E. coli* proteins. Microbiome studies are rapidly unveiling the importance of commensal bacteria to the health of all higher organisms. Our findings in this model commensal organism provide insights into how chronic mercury exposure might affect such complex microbial communities and, consequently, the health of the host. This work also serves as a foundation for studies now underway of how the widely found mobile Hg resistance (*mer*) locus assists the cell in recovery from Hg exposure.

LIST OF ABBREVIATIONS:

Hg = mercury

$HgCl_2$ = mercuric chloride

PMA = phenylmercuric acetate

PhHg = phenylmercury

DMSO = dimethyl sulfoxide

LB = Luria-Bertani medium

NM3 = Neidhardt MOPS minimal medium

NGS = next generation sequencing

DEGs = differentially expressed genes

CVAA = cold vapor atomic absorption

GSH = glutathione

Cys = cysteine

MDR = multidrug resistance

ncRNA = non-coding RNA

COGs = clusters of orthologous groups

GOFs = gene-ontology functions

RNAP = RNA polymerase

HSP = heat shock protein

ETC = electron transport chain

PGA = poly-β-1,6-N-acetyl-glucosamine

DECLARATIONS

Ethics approval and consent to participate: Not applicable

Consent for publication: Not applicable

Availability of data and materials: The tabulated datasets supporting the conclusions of this article are included as additional files. The read counts and raw sequence data (.fastq) are stored and available to the public through the Gene Expression Omnibus database (http://www.ncbi.nlm.nih.gov/geo/) with accession ID: GSE95575.

Competing interest: The authors declare that they have no competing interests.

Funding: US Department of Energy awards ER64408 and ER65286 to AOS

Authors' contributions: SL conceived and designed experiments, prepared biological samples, extracted ribosomal depleted RNA for RNA-Seq, performed all data analysis, and drafted manuscript. AOS was a major contributor in experimental design, feedback

on data analysis, and in editing the manuscript. All authors read and approved the manuscript.

ACKNOWLEDGMENTS

We thank Roger Nilsen at the Georgia Genomics Facility for library preparation and Sharron Crane at Rutgers University for Hg content analysis. We also thank Bryndan Durham, Brandon Satinsky, Mary Ann Moran, Michael K. Johnson, Harry Dailey, Timothy Hoover, Anna Karls, Alexander Johs, Jerry Parks, Susan Miller, and Andrew Wiggins who have provided feedback and discussion on this work. This work was supported by US Department of Energy awards ER64408 and ER65286 to AOS.

REFERENCES

1. Driscoll CT, Mason RP, Chan HM, Jacob DJ, Pirrone N. Mercury as a global pollutant: sources, pathways, and effects. *Environ Sci Technol.* 2013;47(10):4967-4983.

2. Pirrone N, Cinnirella S, Feng X, Finkelman RB, Friedli HR, Leaner J, Mason R, Mukherjee AB, Stracher G, Streets DG *et al*: Global Mercury Emissions to the Atmosphere from Natural and Anthropogenic Sources. In: Mason R, Pirrone N, editors. *Mercury Fate and Transport in the Global Atmosphere: Emissions, Measurements and Models.* Boston, MA: Springer US;2009. p. 1-47.

3. Mason RP, Fitzgerald WF, Morel FMM. The Biogeochemical Cycling of Elemental Mercury - Anthropogenic Influences. *Geochimica Et Cosmochimica Acta.* 1994;58:3191-3198.

4. Barkay T, Miller SM, Summers AO. Bacterial mercury resistance from atoms to ecosystems. *FEMS Microbiol Rev.* 2003;27(2-3):355-384.

5. Crinnion WJ. Environmental medicine, part three: long-term effects of chronic low-dose mercury exposure. *Altern Med Rev.* 2000;5(3):209-223.

6. Richardson GM, Wilson R, Allard D, Purtill C, Douma S, Graviere J. Mercury exposure and risks from dental amalgam in the US population, post-2000. *The Science of the total environment.* 2011;409(20):4257-4268.

7. Diez S. Human health effects of methylmercury exposure. *Rev Environ Contam Toxicol.* 2009;198:111-132.

8. Malm O. Gold mining as a source of mercury exposure in the Brazilian Amazon. *Environ Res.* 1998;77(2):73-78.

9. Clarkson TW, Magos L. The toxicology of mercury and its chemical compounds. *Crit Rev Toxicol.* 2006;36(8):609-662.

10. Hintelmann H, Hempel M, Wilken RD. Observation of unusual organic mercury species in soils and sediments of industrially contaminated sites. *Environ Sci Technol.* 1995;29(7):1845-1850.

11. Tchounwou PB, Ayensu WK, Ninashvili N, Sutton D. Environmental exposure to mercury and its toxicopathologic implications for public health. *Environ Toxicol.* 2003;18(3):149-175.

12. Davidson PW, Myers GJ, Weiss B. Mercury exposure and child development outcomes. *Pediatrics.* 2004;113(Suppl 4):1023-1029.

13. Valko M, Morris H, Cronin MT. Metals, toxicity and oxidative stress. *Curr Med Chem.* 2005;12(10):1161-1208.

14. Yorifuji T, Tsuda T, Takao S, Harada M. Long-term exposure to methylmercury and neurologic signs in Minamata and neighboring communities. *Epidemiology.* 2008;19(1):3-9.

15. Zahir F, Rizwi SJ, Haq SK, Khan RH. Low dose mercury toxicity and human health. *Environ Toxicol Pharmacol.* 2005;20(2):351-360.

16. Cheesman BV, Arnold AP, Rabenstein DL. Nuclear magnetic resonance studies of the solution chemistry of metal complexes. 25. Hg(thiol)3 complexes and HG(II)-thiol ligand exchange kinetics. *J Am Chem Soc.* 1988;110:6359-6364.

17. Oram PD, Fang X, Fernando Q, Letkeman P, Letkeman D. The formation of constants of mercury(II)--glutathione complexes. *Chemical research in toxicology.* 1996;9(4):709-712.

18. Labunskyy VM, Hatfield DL, Gladyshev VN. Selenoproteins: molecular pathways and physiological roles. *Physiol Rev.* 2014;94(3):739-777.

19. Pal PB, Pal S, Das J, Sil PC. Modulation of mercury-induced mitochondria-dependent apoptosis by glycine in hepatocytes. *Amino Acids.* 2012;42(5):1669-1683.

20. Shenker BJ, Guo TL, Shapiro IM. Mercury-induced apoptosis in human lymphoid cells: evidence that the apoptotic pathway is mercurial species dependent. *Environ Res.* 2000;84(2):89-99.

21. Jomova K, Valko M. Advances in metal-induced oxidative stress and human disease. *Toxicology.* 2011;283(2-3):65-87.

22. Polacco BJ, Purvine SO, Zink EM, Lavoie SP, Lipton MS, Summers AO, Miller SM. Discovering mercury protein modifications in whole proteomes using natural isotope distributions observed in liquid chromatography-tandem mass spectrometry. *Mol Cell Proteomics.* 2011;10(8):M110.004853.

23. LaVoie SP, Mapolelo DT, Cowart DM, Polacco BJ, Johnson MK, Scott RA, Miller SM, Summers AO. Organic and inorganic mercurials have distinct effects on cellular thiols, metal homeostasis, and Fe-binding proteins in Escherichia coli. *J Biol Inorg Chem.* 2015;20(8):1239-1251.

24. McElwee MK, Ho LA, Chou JW, Smith MV, Freedman JH. Comparative toxicogenomic responses of mercuric and methyl-mercury. *BMC Genomics.* 2013;14:698.

25. Neidhardt FC, Bloch PL, Smith DF. Culture medium for enterobacteria. *J Bacteriol.* 1974;119(3):736-747.

26. Stead MB, Agrawal A, Bowden KE, Nasir R, Mohanty BK, Meagher RB, Kushner SR. RNAsnap: a rapid, quantitative and inexpensive, method for isolating total RNA from bacteria. *Nucleic acids research.* 2012;40(20):e156.

27. Langmead B, Salzberg SL. Fast gapped-read alignment with Bowtie 2. *Nature methods.* 2012;9(4):357-359.

28. Li H, Handsaker B, Wysoker A, Fennell T, Ruan J, Homer N, Marth G, Abecasis G, Durbin R, Genome Project Data Processing S. The Sequence Alignment/Map format and SAMtools. *Bioinformatics.* 2009;25(16):2078-2079.

29. Anders S, Pyl PT, Huber W. HTSeq--a Python framework to work with high-throughput sequencing data. *Bioinformatics.* 2015;31(2):166-169.

30. Hardcastle TJ, Kelly KA. baySeq: empirical Bayesian methods for identifying differential expression in sequence count data. *BMC bioinformatics.* 2010;11:422.

31. Hamlett NV, Landale EC, Davis BH, Summers AO. Roles of the Tn21 merT, merP, and merC gene products in mercury resistance and mercury binding. *J Bacteriol.* 1992;174(20):6377-6385.

32. Summers AO, Lewis E. Volatilization of mercuric chloride by mercury-resistant plasmid-bearing strains of Escherichia coli, Staphylococcus aureus, and Pseudomonas aeruginosa. *J Bacteriol.* 1973;113(2):1070-1072.

1175 33. Summers AO, Silver S. Mercury resistance in a plasmid-bearing strain of
1176 Escherichia coli. *J Bacteriol.* 1972;112(3):1228-1236.

1177 34. Schaechter M, Santomassino KA. Lysis of Escherichia coli by sulfhydryl-binding
1178 reagents. *J Bacteriol.* 1962;84:318-325.

1179 35. Janssen BD, Hayes CS. The tmRNA ribosome-rescue system. *Adv Protein Chem*
1180 *Struct Biol.* 2012;86:151-191.

1181 36. Legendre P. Ward's Hierarchical Agglomerative Clustering Method: Which
1182 Algorithms Implement Ward's Criterion? *Journal of Classification.* 2014;31(3):274-
1183 295.

1184 37. Szklarczyk D, Franceschini A, Wyder S, Forslund K, Heller D, Huerta-Cepas J,
1185 Simonovic M, Roth A, Santos A, Tsafou KP *et al*. STRING v10: protein-protein
1186 interaction networks, integrated over the tree of life. *Nucleic acids research.*
1187 2015;43(Database issue):D447-452.

1188 38. von Mering C, Jensen LJ, Snel B, Hooper SD, Krupp M, Foglierini M, Jouffre N,
1189 Huynen MA, Bork P. STRING: known and predicted protein-protein associations,
1190 integrated and transferred across organisms. *Nucleic acids research.*
1191 2005;33(Database issue):D433-437.

1192 39. Arunasri K, Adil M, Khan PA, Shivaji S. Global gene expression analysis of long-
1193 term stationary phase effects in E. coli K12 MG1655. *PLoS One.*
1194 2014;9(5):e96701.

1195 40. Chang DE, Smalley DJ, Conway T. Gene expression profiling of Escherichia coli
1196 growth transitions: an expanded stringent response model. *Mol Microbiol.*
1197 2002;45(2):289-306.

1198 41. Kuzminov A. Recombinational repair of DNA damage in Escherichia coli and
1199 bacteriophage lambda. *Microbiol Mol Biol Rev.* 1999;63(4):751-813.

1200 42. Lusetti SL, Cox MM. The bacterial RecA protein and the recombinational DNA
1201 repair of stalled replication forks. *Annu Rev Biochem.* 2002;71:71-100.

1202 43. Salgado H, Martinez-Flores I, Lopez-Fuentes A, Garcia-Sotelo JS, Porron-Sotelo
1203 L, Solano H, Muniz-Rascado L, Collado-Vides J. Extracting regulatory networks of
1204 Escherichia coli from RegulonDB. *Methods Mol Biol.* 2012;804:179-195.

1205 44. Salgado H, Peralta-Gil M, Gama-Castro S, Santos-Zavaleta A, Muniz-Rascado L,
1206 Garcia-Sotelo JS, Weiss V, Solano-Lira H, Martinez-Flores I, Medina-Rivera A *et*
1207 *al*. RegulonDB v8.0: omics data sets, evolutionary conservation, regulatory
1208 phrases, cross-validated gold standards and more. *Nucleic acids research.*
1209 2013;41(Database issue):D203-213.

45. Tramonti A, Visca P, De Canio M, Falconi M, De Biase D. Functional characterization and regulation of gadX, a gene encoding an AraC/XylS-like transcriptional activator of the Escherichia coli glutamic acid decarboxylase system. *J Bacteriol.* 2002;184(10):2603-2613.

46. Nishino K, Senda Y, Yamaguchi A. The AraC-family regulator GadX enhances multidrug resistance in Escherichia coli by activating expression of mdtEF multidrug efflux genes. *J Infect Chemother.* 2008;14(1):23-29.

47. Tucker DL, Tucker N, Ma Z, Foster JW, Miranda RL, Cohen PS, Conway T. Genes of the GadX-GadW regulon in Escherichia coli. *J Bacteriol.* 2003;185(10):3190-3201.

48. Lemke JJ, Sanchez-Vazquez P, Burgos HL, Hedberg G, Ross W, Gourse RL. Direct regulation of Escherichia coli ribosomal protein promoters by the transcription factors ppGpp and DksA. *Proc Natl Acad Sci U S A.* 2011;108(14):5712-5717.

49. Nomura M, Gourse R, Baughman G. Regulation of the synthesis of ribosomes and ribosomal components. *Annu Rev Biochem.* 1984;53:75-117.

50. Wilson DN, Nierhaus KH. The weird and wonderful world of bacterial ribosome regulation. *Crit Rev Biochem Mol Biol.* 2007;42(3):187-219.

51. Soskine M, Steiner-Mordoch S, Schuldiner S. Crosslinking of membrane-embedded cysteines reveals contact points in the EmrE oligomer. *Proc Natl Acad Sci U S A.* 2002;99(19):12043-12048.

52. Imesch E, Moosmayer M, Anner BM. Mercury weakens membrane anchoring of Na-K-ATPase. *The American journal of physiology.* 1992;262(5):F837-842.

53. Carvalho CM, Chew EH, Hashemy SI, Lu J, Holmgren A. Inhibition of the human thioredoxin system. A molecular mechanism of mercury toxicity. *The Journal of biological chemistry.* 2008;283(18):11913-11923.

54. Georgopoulos C, Welch WJ. Role of the major heat shock proteins as molecular chaperones. *Annu Rev Cell Biol.* 1993;9:601-634.

55. Carpousis AJ. The RNA degradosome of Escherichia coli: an mRNA-degrading machine assembled on RNase E. *Annu Rev Microbiol.* 2007;61:71-87.

56. Lim JY, May JM, Cegelski L. Dimethyl sulfoxide and ethanol elicit increased amyloid biogenesis and amyloid-integrated biofilm formation in Escherichia coli. *Appl Environ Microbiol.* 2012;78(9):3369-3378.

57. Markarian SA, Poladyan AA, Kirakosyan GR, Trchounian AA, Bagramyan KA. Effect of diethylsulphoxide on growth, survival and ion exchange of Escherichia coli. *Lett Appl Microbiol.* 2002;34(6):417-421.

1246 58. Ansaldi M, Bordi C, Lepelletier M, Mejean V. TorC apocytochrome negatively
1247 autoregulates the trimethylamine N-oxide (TMAO) reductase operon in Escherichia
1248 coli. *Mol Microbiol.* 1999;33(2):284-295.

1249 59. Sorensen KI, Hove-Jensen B. Ribose catabolism of Escherichia coli:
1250 characterization of the rpiB gene encoding ribose phosphate isomerase B and of
1251 the rpiR gene, which is involved in regulation of rpiB expression. *J Bacteriol.*
1252 1996;178(4):1003-1011.

1253 60. Yamada T, Letunic I, Okuda S, Kanehisa M, Bork P. iPath2.0: interactive pathway
1254 explorer. *Nucleic acids research.* 2011;39(Web Server issue):W412-415.

1255 61. Imlay JA. The molecular mechanisms and physiological consequences of oxidative
1256 stress: lessons from a model bacterium. *Nat Rev Microbiol.* 2013;11(7):443-454.

1257 62. Grass G, Otto M, Fricke B, Haney CJ, Rensing C, Nies DH, Munkelt D. FieF (YiiP)
1258 from Escherichia coli mediates decreased cellular accumulation of iron and
1259 relieves iron stress. *Arch Microbiol.* 2005;183(1):9-18.

1260 63. Bandyopadhyay S, Chandramouli K, Johnson MK. Iron-sulfur cluster biosynthesis.
1261 *Biochem Soc Trans.* 2008;36(Pt 6):1112-1119.

1262 64. Johnson DC, Dean DR, Smith AD, Johnson MK. Structure, function, and formation
1263 of biological iron-sulfur clusters. *Annu Rev Biochem.* 2005;74:247-281.

1264 65. Rensing C, Mitra B, Rosen BP. The zntA gene of Escherichia coli encodes a Zn(II)-
1265 translocating P-type ATPase. *Proc Natl Acad Sci U S A.* 1997;94(26):14326-
1266 14331.

1267 66. Outten FW, Huffman DL, Hale JA, O'Halloran TV. The independent cue and cus
1268 systems confer copper tolerance during aerobic and anaerobic growth in
1269 Escherichia coli. *The Journal of biological chemistry.* 2001;276(33):30670-30677.

1270 67. Eitinger T, Mandrand-Berthelot MA. Nickel transport systems in microorganisms.
1271 *Arch Microbiol.* 2000;173(1):1-9.

1272 68. Qin J, Fu HL, Ye J, Bencze KZ, Stemmler TL, Rawlings DE, Rosen BP.
1273 Convergent evolution of a new arsenic binding site in the ArsR/SmtB family of
1274 metalloregulators. *The Journal of biological chemistry.* 2007;282(47):34346-34355.

1275 69. Alekshun MN, Levy SB. The mar regulon: multiple resistance to antibiotics and
1276 other toxic chemicals. *Trends Microbiol.* 1999;7(10):410-413.

1277 70. Nishino K, Yamada J, Hirakawa H, Hirata T, Yamaguchi A. Roles of TolC-
1278 dependent multidrug transporters of Escherichia coli in resistance to beta-lactams.
1279 *Antimicrob Agents Chemother.* 2003;47(9):3030-3033.

71. Raetz CR, Reynolds CM, Trent MS, Bishop RE. Lipid A modification systems in gram-negative bacteria. *Annu Rev Biochem.* 2007;76:295-329.

72. Checroun C, Gutierrez C. Sigma(s)-dependent regulation of yehZYXW, which encodes a putative osmoprotectant ABC transporter of Escherichia coli. *FEMS Microbiol Lett.* 2004;236(2):221-226.

73. Van Houdt R, Michiels CW. Role of bacterial cell surface structures in Escherichia coli biofilm formation. *Res Microbiol.* 2005;156(5-6):626-633.

74. Ma Q, Zhang G, Wood TK. Escherichia coli BdcA controls biofilm dispersal in Pseudomonas aeruginosa and Rhizobium meliloti. *BMC Res Notes.* 2011;4:447.

75. Zhang XS, Garcia-Contreras R, Wood TK. YcfR (BhsA) influences Escherichia coli biofilm formation through stress response and surface hydrophobicity. *J Bacteriol.* 2007;189(8):3051-3062.

76. Itoh Y, Rice JD, Goller C, Pannuri A, Taylor J, Meisner J, Beveridge TJ, Preston JF, 3rd, Romeo T. Roles of pgaABCD genes in synthesis, modification, and export of the Escherichia coli biofilm adhesin poly-beta-1,6-N-acetyl-D-glucosamine. *J Bacteriol.* 2008;190(10):3670-3680.

77. Lee J, Page R, Garcia-Contreras R, Palermino JM, Zhang XS, Doshi O, Wood TK, Peti W. Structure and function of the Escherichia coli protein YmgB: a protein critical for biofilm formation and acid-resistance. *J Mol Biol.* 2007;373(1):11-26.

78. Cegelski L, Pinkner JS, Hammer ND, Cusumano CK, Hung CS, Chorell E, Aberg V, Walker JN, Seed PC, Almqvist F *et al*. Small-molecule inhibitors target Escherichia coli amyloid biogenesis and biofilm formation. *Nat Chem Biol.* 2009;5(12):913-919.

79. Seo SW, Kim D, Szubin R, Palsson BO. Genome-wide Reconstruction of OxyR and SoxRS Transcriptional Regulatory Networks under Oxidative Stress in Escherichia coli K-12 MG1655. *Cell Rep.* 2015;12(8):1289-1299.

80. Choi H, Kim S, Mukhopadhyay P, Cho S, Woo J, Storz G, Ryu SE. Structural basis of the redox switch in the OxyR transcription factor. *Cell.* 2001;105(1):103-113.

81. Altuvia S, Zhang A, Argaman L, Tiwari A, Storz G. The Escherichia coli OxyS regulatory RNA represses fhlA translation by blocking ribosome binding. *EMBO J.* 1998;17(20):6069-6075.

82. Amabile-Cuevas CF, Demple B. Molecular characterization of the soxRS genes of Escherichia coli: two genes control a superoxide stress regulon. *Nucleic acids research.* 1991;19(16):4479-4484.

1314 83. Greenberg JT, Monach P, Chou JH, Josephy PD, Demple B. Positive control of a
1315 global antioxidant defense regulon activated by superoxide-generating agents in
1316 Escherichia coli. *Proc Natl Acad Sci U S A.* 1990;87(16):6181-6185.

1317 84. Tsaneva IR, Weiss B. soxR, a locus governing a superoxide response regulon in
1318 Escherichia coli K-12. *J Bacteriol.* 1990;172(8):4197-4205.

1319 85. Watanabe S, Kita A, Kobayashi K, Miki K. Crystal structure of the [2Fe-2S]
1320 oxidative-stress sensor SoxR bound to DNA. *Proc Natl Acad Sci U S A.*
1321 2008;105(11):4121-4126.

1322 86. Keseler IM, Mackie A, Peralta-Gil M, Santos-Zavaleta A, Gama-Castro S,
1323 Bonavides-Martinez C, Fulcher C, Huerta AM, Kothari A, Krummenacker M *et al*.
1324 EcoCyc: fusing model organism databases with systems biology. *Nucleic acids*
1325 *research.* 2013;41(Database issue):D605-612.

1326 87. Anjem A, Varghese S, Imlay JA. Manganese import is a key element of the OxyR
1327 response to hydrogen peroxide in Escherichia coli. *Mol Microbiol.* 2009;72(4):844-
1328 858.

1329 88. Park SJ, Gunsalus RP. Oxygen, iron, carbon, and superoxide control of the
1330 fumarase fumA and fumC genes of Escherichia coli: role of the arcA, fnr, and soxR
1331 gene products. *J Bacteriol.* 1995;177(21):6255-6262.

1332 89. Varghese S, Tang Y, Imlay JA. Contrasting sensitivities of Escherichia coli
1333 aconitases A and B to oxidation and iron depletion. *J Bacteriol.* 2003;185(1):221-
1334 230.

1335 90. Eser M, Masip L, Kadokura H, Georgiou G, Beckwith J. Disulfide bond formation
1336 by exported glutaredoxin indicates glutathione's presence in the E. coli periplasm.
1337 *Proc Natl Acad Sci U S A.* 2009;106(5):1572-1577.

1338 91. Suzuki H, Koyanagi T, Izuka S, Onishi A, Kumagai H. The yliA, -B, -C, and -D
1339 genes of Escherichia coli K-12 encode a novel glutathione importer with an ATP-
1340 binding cassette. *J Bacteriol.* 2005;187(17):5861-5867.

1341 92. Vuilleumier S. Bacterial glutathione S-transferases: what are they good for? *J*
1342 *Bacteriol.* 1997;179(5):1431-1441.

1343 93. Summers AO, Wireman J, Vimy MJ, Lorscheider FL, Marshall B, Levy SB, Bennett
1344 S, Billard L. Mercury released from dental "silver" fillings provokes an increase in
1345 mercury- and antibiotic-resistant bacteria in oral and intestinal floras of primates.
1346 *Antimicrob Agents Chemother.* 1993;37(4):825-834.

1347 94. US - Food & Drug Administration (FDA): Mercury Levels in Commercial Fish and
1348 Shellfish (1990-2012)
1349 http://www.fda.gov/Food/FoodborneIllnessContaminants/Metals/ucm115644.htm

95. McElwee MK, Freedman JH. Comparative toxicology of mercurials in Caenorhabditis elegans. *Environ Toxicol Chem.* 2011;30(9):2135-2141.

96. Zheng M, Wang X, Templeton LJ, Smulski DR, LaRossa RA, Storz G. DNA microarray-mediated transcriptional profiling of the Escherichia coli response to hydrogen peroxide. *J Bacteriol.* 2001;183(15):4562-4570.

97. Mehta HH, Liu Y, Zhang MQ, Spiro S. Genome-wide analysis of the response to nitric oxide in uropathogenic Escherichia coli CFT073. *Microb Genom.* 2015;1(4):e000031.

98. Rau MH, Calero P, Lennen RM, Long KS, Nielsen AT. Genome-wide Escherichia coli stress response and improved tolerance towards industrially relevant chemicals. *Microb Cell Fact.* 2016;15(1):176.

99. Yung PY, Grasso LL, Mohidin AF, Acerbi E, Hinks J, Seviour T, Marsili E, Lauro FM. Global transcriptomic responses of Escherichia coli K-12 to volatile organic compounds. *Sci Rep.* 2016;6:19899.

100. Wong GT, Bonocora RP, Schep AN, Beeler SM, Lee Fong AJ, Shull LM, Batachari LE, Dillon M, Evans C, Becker CJ *et al*. Genome-Wide Transcriptional Response to Varying RpoS Levels in Escherichia coli K-12. *J Bacteriol.* 2017;199(7).

101. Ung CY, Lam SH, Hlaing MM, Winata CL, Korzh S, Mathavan S, Gong Z. Mercury-induced hepatotoxicity in zebrafish: in vivo mechanistic insights from transcriptome analysis, phenotype anchoring and targeted gene expression validation. *BMC Genomics.* 2010;11:212.

102. Lash LH, Zalups RK. Alterations in renal cellular glutathione metabolism after in vivo administration of a subtoxic dose of mercuric chloride. *J Biochem Toxicol.* 1996;11(1):1-9.

103. Lu X, Xiang Y, Yang G, Zhang L, Wang H, Zhong S. Transcriptomic characterization of zebrafish larvae in response to mercury exposure. *Comp Biochem Physiol C Toxicol Pharmacol.* 2017;192:40-49.

104. Kanai T, Takahashi K, Inoue H. Three distinct-type glutathione S-transferases from Escherichia coli important for defense against oxidative stress. *J Biochem.* 2006;140(5):703-711.

105. Xu FF, Imlay JA. Silver(I), mercury(II), cadmium(II), and zinc(II) target exposed enzymic iron-sulfur clusters when they toxify Escherichia coli. *Appl Environ Microbiol.* 2012;78(10):3614-3621.

106. Varghese S, Wu A, Park S, Imlay KR, Imlay JA. Submicromolar hydrogen peroxide disrupts the ability of Fur protein to control free-iron levels in Escherichia coli. *Mol Microbiol.* 2007;64(3):822-830.

1386 107. Bagg A, Neilands JB. Ferric uptake regulation protein acts as a repressor,
1387 employing iron (II) as a cofactor to bind the operator of an iron transport operon in
1388 Escherichia coli. *Biochemistry.* 1987;26(17):5471-5477.

1389 108. de Lorenzo V, Wee S, Herrero M, Neilands JB. Operator sequences of the
1390 aerobactin operon of plasmid ColV-K30 binding the ferric uptake regulation (fur)
1391 repressor. *J Bacteriol.* 1987;169(6):2624-2630.

1392 109. Fontecave M, Choudens SO, Py B, Barras F. Mechanisms of iron-sulfur cluster
1393 assembly: the SUF machinery. *J Biol Inorg Chem.* 2005;10(7):713-721.

1394 110. Zhao G, Ceci P, Ilari A, Giangiacomo L, Laue TM, Chiancone E, Chasteen ND.
1395 Iron and hydrogen peroxide detoxification properties of DNA-binding protein from
1396 starved cells. A ferritin-like DNA-binding protein of Escherichia coli. *The Journal of*
1397 *biological chemistry.* 2002;277(31):27689-27696.

1398 111. Lund BO, Miller DM, Woods JS. Mercury-induced H2O2 production and lipid
1399 peroxidation in vitro in rat kidney mitochondria. *Biochem Pharmacol.* 1991;42
1400 Suppl:S181-187.

1401 112. Liochev SI, Fridovich I. Modulation of the fumarases of Escherichia coli in
1402 response to oxidative stress. *Arch Biochem Biophys.* 1993;301(2):379-384.

1403 113. Martin JE, Imlay JA. The alternative aerobic ribonucleotide reductase of
1404 Escherichia coli, NrdEF, is a manganese-dependent enzyme that enables cell
1405 replication during periods of iron starvation. *Mol Microbiol.* 2011;80(2):319-334.

1406 114. Jordan A, Aslund F, Pontis E, Reichard P, Holmgren A. Characterization of
1407 Escherichia coli NrdH. A glutaredoxin-like protein with a thioredoxin-like activity
1408 profile. *The Journal of biological chemistry.* 1997;272(29):18044-18050.

1409 115. Sharma SK, Goloubinoff P, Christen P. Heavy metal ions are potent inhibitors of
1410 protein folding. *Biochem Biophys Res Commun.* 2008;372(2):341-345.

1411 116. Arsene F, Tomoyasu T, Bukau B. The heat shock response of Escherichia coli. *Int*
1412 *J Food Microbiol.* 2000;55(1-3):3-9.

1413 117. Bissonnette SA, Rivera-Rivera I, Sauer RT, Baker TA. The IbpA and IbpB small
1414 heat-shock proteins are substrates of the AAA+ Lon protease. *Mol Microbiol.*
1415 2010;75(6):1539-1549.

1416 118. Gaubig LC, Waldminghaus T, Narberhaus F. Multiple layers of control govern
1417 expression of the Escherichia coli ibpAB heat-shock operon. *Microbiology.*
1418 2011;157(Pt 1):66-76.

1419 119. Matuszewska E, Kwiatkowska J, Kuczynska-Wisnik D, Laskowska E. Escherichia
1420 coli heat-shock proteins IbpA/B are involved in resistance to oxidative stress
1421 induced by copper. *Microbiology.* 2008;154(Pt 6):1739-1747.

120. Wang A, Crowley DE. Global gene expression responses to cadmium toxicity in Escherichia coli. *J Bacteriol.* 2005;187(9):3259-3266.

121. Salmon K, Hung SP, Mekjian K, Baldi P, Hatfield GW, Gunsalus RP. Global gene expression profiling in Escherichia coli K12. The effects of oxygen availability and FNR. *The Journal of biological chemistry.* 2003;278(32):29837-29855.

122. Bibikov SI, Biran R, Rudd KE, Parkinson JS. A signal transducer for aerotaxis in Escherichia coli. *J Bacteriol.* 1997;179(12):4075-4079.

123. Pruss BM, Campbell JW, Van Dyk TK, Zhu C, Kogan Y, Matsumura P. FlhD/FlhC is a regulator of anaerobic respiration and the Entner-Doudoroff pathway through induction of the methyl-accepting chemotaxis protein Aer. *J Bacteriol.* 2003;185(2):534-543.

124. Funk AE, Day FA, Brady FO. Displacement of zinc and copper from copper-induced metallothionein by cadmium and by mercury: in vivo and ex vivo studies. *Comp Biochem Physiol C.* 1987;86(1):1-6.

125. O'Connor TR, Graves RJ, de Murcia G, Castaing B, Laval J. Fpg protein of Escherichia coli is a zinc finger protein whose cysteine residues have a structural and/or functional role. *The Journal of biological chemistry.* 1993;268(12):9063-9070.

126. Binet MR, Poole RK. Cd(II), Pb(II) and Zn(II) ions regulate expression of the metal-transporting P-type ATPase ZntA in Escherichia coli. *FEBS Lett.* 2000;473(1):67-70.

127. Petit-Hartlein I, Rome K, de Rosny E, Molton F, Duboc C, Gueguen E, Rodrigue A, Coves J. Biophysical and physiological characterization of ZraP from Escherichia coli, the periplasmic accessory protein of the atypical ZraSR two-component system. *Biochem J.* 2015;472(2):205-216.

128. Colaco HG, Santo PE, Matias PM, Bandeiras TM, Vicente JB. Roles of Escherichia coli ZinT in cobalt, mercury and cadmium resistance and structural insights into the metal binding mechanism. *Metallomics.* 2016;8(3):327-336.

129. Owens RA, Hartman PE. Export of glutathione by some widely used Salmonella typhimurium and Escherichia coli strains. *J Bacteriol.* 1986;168(1):109-114.

130. Smirnova GV, Muzyka NG, Oktyabrsky ON. Effects of cystine and hydrogen peroxide on glutathione status and expression of antioxidant genes in Escherichia coli. *Biochemistry (Mosc).* 2005;70(8):926-934.

131. Fitzgerald DM, Bonocora RP, Wade JT. Comprehensive mapping of the Escherichia coli flagellar regulatory network. *PLoS Genet.* 2014;10(10):e1004649.

132. Dong T, Yu R, Schellhorn H. Antagonistic regulation of motility and transcriptome expression by RpoN and RpoS in Escherichia coli. *Mol Microbiol.* 2011;79(2):375-386.

133. De Lay N, Gottesman S. A complex network of small non-coding RNAs regulate motility in Escherichia coli. *Mol Microbiol.* 2012;86(3):524-538.

134. Mermod M, Magnani D, Solioz M, Stoyanov JV. The copper-inducible ComR (YcfQ) repressor regulates expression of ComC (YcfR), which affects copper permeability of the outer membrane of Escherichia coli. *Biometals.* 2012;25(1):33-43.

135. Schwechheimer C, Kuehn MJ. Outer-membrane vesicles from Gram-negative bacteria: biogenesis and functions. *Nat Rev Microbiol.* 2015;13(10):605-619.

136. Crepin S, Chekabab SM, Le Bihan G, Bertrand N, Dozois CM, Harel J. The Pho regulon and the pathogenesis of Escherichia coli. *Vet Microbiol.* 2011;153(1-2):82-88.

137. Hsieh YJ, Wanner BL. Global regulation by the seven-component Pi signaling system. *Curr Opin Microbiol.* 2010;13(2):198-203.

138. Hondorp ER, Matthews RG. Oxidative stress inactivates cobalamin-independent methionine synthase (MetE) in Escherichia coli. *PLoS Biol.* 2004;2(11):e336.

139. Brooks P, Davidson N. Mercury(II) Complexes of Imidazole and Histidine. *Journal of the American Chemical Society.* 1960;82(9):2118-2123.

140. Pal C, Bengtsson-Palme J, Kristiansson E, Larsson DG. Co-occurrence of resistance genes to antibiotics, biocides and metals reveals novel insights into their co-selection potential. *BMC Genomics.* 2015;16(1):964.

141. Wireman J, Liebert CA, Smith T, Summers AO. Association of mercury resistance with antibiotic resistance in the gram-negative fecal bacteria of primates. *Appl Environ Microbiol.* 1997;63(11):4494-4503.

142. Mehta P, Casjens S, Krishnaswamy S. Analysis of the lambdoid prophage element e14 in the E. coli K-12 genome. *BMC Microbiol.* 2004;4:4.

143. Wang X, Kim Y, Ma Q, Hong SH, Pokusaeva K, Sturino JM, Wood TK. Cryptic prophages help bacteria cope with adverse environments. *Nat Commun.* 2010;1:147.

Table 1: Genes with ≥ 20 fold-change for at least two time points after $HgCl_2$ exposure (n = 25).

Gene ID	Gene Name	Product Description	Hg t10	Hg t30	Hg t60	PMA t10	PMA t30	PMA t60
b1112	**bhsA**	Biofilm, cell surface and signaling defects, YhcN family	**1949**	**563**	**94**	**46**	**21**	n.s.
b4458	oxyS	OxyS sRNA activates genes that detoxify oxidative damage	**1524**	**1292**	**150**	10	6	n.s.
b4249	bdcA	c-di-GMP-binding biofilm dispersal mediator protein	**596**	**79**	7	16	2	n.s.
b3686	**ibpB**	Chaperone, heat-inducible protein of HSP20 family	**402**	**124**	**281**	**37**	**211**	9
b0812	dps	Stress-induced Fe-binding and storage protein	**339**	**52**	n.s.	4	2	n.s.
b4248	yjgH	Putative reactive intermediate deaminase, UPF0076 family	**296**	**24**	3	6	2	n.s.
b0849	grxA	Glutaredoxin 1	**246**	**33**	n.s.	14	4	n.s.
b1144	ymfJ	Function unknown, e14 prophage	**185**	**39**	n.s.	3	3	n.s.
b2582	**trxC**	Thioredoxin 2, zinc-binding; Trx2	**134**	**50**	7	**24**	**24**	n.s.
b1147	ymfL*	Function unknown, e14 prophage	**95**	**29**	n.s.	n.s.	3	n.s.
b1146	croE*	Cro-like repressor, e14 prophage	**90**	**40**	n.s.	n.s.	n.s.	n.s.
b3687	**ibpA**	Chaperone, heat-inducible protein of HSP20 family	**86**	19	**41**	10	**28**	4
b2531	iscR	Transcriptional repressor for isc operon; contains Fe-S cluster	**62**	**48**	9	12	18	n.s.
b1148	ymfM*	Function unknown, e14 prophage	**49**	**21**	n.s.	n.s.	n.s.	n.s.
b4599	yneM	function unknown, membrane-associated; regulated by PhoPQ	**38**	**36**	n.s.	3	3	n.s.
b2673	nrdH	NrdH-redoxin reducing oxidized NrdEF	**35**	**127**	**21**	7	14	n.s.
b4030	**psiE**	Pho regulon, regulated by phoB and cAMP	**35**	**64**	17	**38**	**59**	n.s.
b1684	sufA	Scaffold protein for assembly of iron-sulfur clusters	**32**	**39**	5	n.s.	3	n.s.
b1748	**astC**	Succinylornithine transaminase; carbon starvation protein	**30**	**31**	**25**	**34**	**36**	n.s.
b4663	**azuC**	Function unknown; membrane-associated	**27**	**25**	**36**	**41**	**49**	n.s.
b0484	copA	Copper-, silver-translocating P-type ATPase efflux pump	**25**	**20**	n.s.	5	n.s.	-10
b2674	nrdI	Flavodoxin required for NrdEF cluster assembly	**21**	**73**	**22**	4	7	n.s.
b1747	astA*	Arginine succinyltransferase, arginine catabolism	10	**20**	**29**	9	14	n.s.
b1020	**phoH**	ATP-binding protein, function unknown	8	**71**	**221**	**61**	**365**	n.s.
b4002	zraP	Zn-dependent periplasmic chaperone	3	**27**	**43**	n.s.	n.s.	-3

Table is sorted by Hg at 10 min column. n.s. = not significantly different from unexposed culture and boldface highlights actual values ≥ 20-fold. Gene names in boldface have a ≥ 20 differential expression response to both Hg and PMA in at least one time point (n = 8). Genes marked with an asterisk (*) had fewer than 11 average read counts for at least 2 time points in the unexposed condition and were operationally defined as being "off" in that condition. Such genes constituted, the lowest 15th percentile of all genes, based on raw read counts normalized across all libraries and across all biological replicates.

Table 2: Genes with ≥ 20 fold-change in at least two time points for PMA exposure (n= 17).

Gene ID	Gene Name	Product Description	Hg t10	Hg t30	Hg t60	PMA t10	PMA t30	PMA t60
b3728	pstS	ABC phosphate transport system; periplasmic binding protein	n.s.	16	8	**86**	**165**	n.s.
b1020	**phoH**	ATP-binding protein, function unknown	8	**71**	**221**	**61**	**365**	n.s.
b0996	torC*	c-Type cytochrome	n.s.	n.s.	n.s.	**55**	**65**	**77**
b4060	**yjcB**	Function unknown	**33**	11	12	**52**	**35**	n.s.
b0399	**phoB**	Positive response regulator for pho regulon	4	**22**	3	**51**	**105**	n.s.
b1530	**marR**	Transcription repressor of multiple antibiotic resistance	**26**	7	n.s.	**48**	**29**	n.s.
b1531	marA	Transcriptional activator for multiple antibiotic resistance;	15	9	n.s.	**46**	**31**	n.s.
b1112	**bhsA**	Biofilm, cell surface and signaling defects, YhcN family	**1949**	**563**	**94**	**46**	**21**	n.s.
b1532	marB	marRAB multiple antibiotic resistance operon	16	8	n.s.	**45**	**27**	n.s.
b4663	**azuC**	Function unknown; membrane-associated	**27**	**25**	**36**	**41**	**49**	n.s.
b4030	**psiE**	Pho regulon, regulated by phoB and cAMP	**35**	**64**	17	**38**	**59**	n.s.
b3686	**ibpB**	Chaperone, heat-inducible protein of HSP20 family	**402**	**124**	**281**	**37**	**211**	9
b1748	**astC**	Succinylornithine transaminase; carbon starvation protein	**30**	**31**	**25**	**34**	**36**	n.s.
b3469	**zntA**	Zn(II), Cd(II), and Pb(II) translocating P-type ATPase	**40**	19	8	**29**	**22**	n.s.
b2582	**trxC**	Thioredoxin 2, zinc-binding; Trx2	**134**	**50**	7	**24**	**24**	n.s.
b4354	yjiY	Predicted transporter, function unknown	n.s.	n.s.	n.s.	**20**	**77**	n.s.
b1625	cnu	OriC-binding complex H-NS/Cnu	n.s.	10	n.s.	**20**	**24**	n.s.

Table is sorted by PMA at 10 min column. n.s. = not significantly different from unexposed culture and boldface highlights actual values ≥ 20-fold. Gene names in boldface have a ≥ 20 differential expression response to both Hg and PMA in at least one time point (n = 11). Genes marked with an asterisk (*) had fewer than 11 average read counts for at least 2 time points in the unexposed condition and were operationally defined as being "off" in that condition. Such genes constituted, the lowest 15th percentile of all genes, based on raw read counts normalized across all libraries and across all biological replicates.

Table 3: Changes in transcription factor gene expression. The sum of transcription factor genes either up-regulated or down-regulated is shown with the percentage of the total transcription factor genes in parenthesis; percents do not total 100 because genes with no change compared to unexposed cells are not tabulated here. See details in Table S12.

Transcription Factors (n = 203)						
	Hg_t10	**Hg_t30**	**Hg_t60**	**PMA_t10**	**PMA_t30**	**PMA_t60**
up	63 (31)	46 (23)	14 (7)	86 (42)	78 (38)	1 (0.5)
down	28 (14)	28 (14)	13 (6)	22 (11)	23 (11)	2 (1)

1525 **Figures**

1526

a

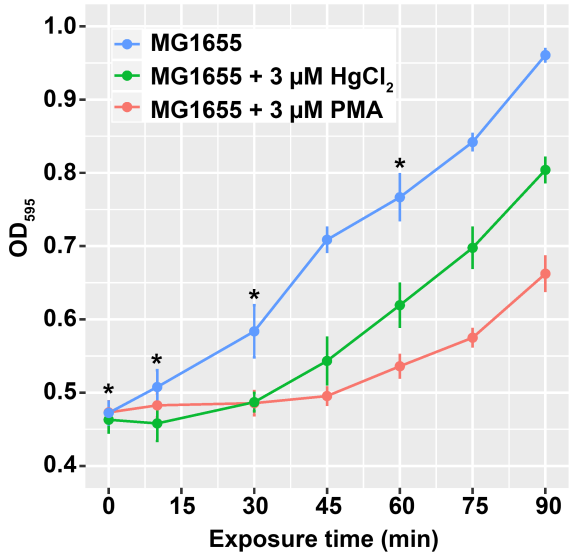

b

	t10	t30	t60
3 µM $HgCl_2$	1,821 (894↑927↓)	1,422 (637↑785↓)	563 (259↑304↓)
3 µM PMA	2,181 (1,261↑920↓)	2,009 (1,156↑853↓)	65 (36↑29↓)

1527

1528 **Figure 1: Effects of sub-acute mercury exposure on growth of MG1655. (a)** *E. coli*
1529 K12 MG1655 grown in MOPS minimal medium, unexposed (blue) or exposed to 3 µM
1530 $HgCl_2$ (red) or 3 µM PMA (green) during mid-log phase. Asterisks indicate sampling
1531 times for RNA-seq. Error bars are standard error (SEM) of 3 biological replicates for
1532 each culture condition. See Figure S1 for full growth curve. **(b)** Significantly differentially
1533 expressed genes (DEG) counts (up-regulated or down-regulated) for $HgCl_2$ and PMA
1534 relative to unexposed control culture at each time point.

1535

1536

1537

1538

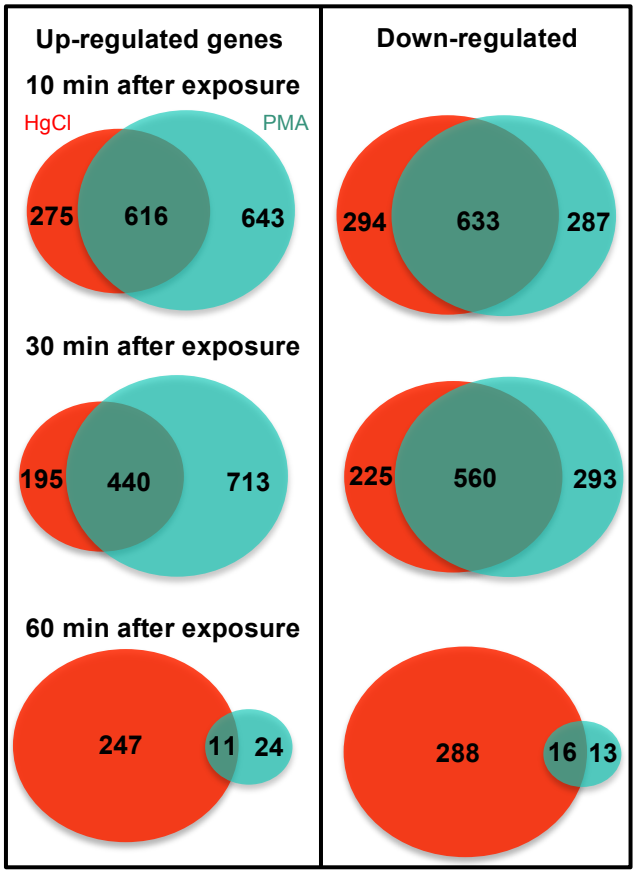

Figure 2: Overlap between differentially expressed genes at each sampling time

The 3 μM $HgCl_2$ exposure is in red and the 3 μM PMA exposure in green. Ovals are to scale only at each time point, but not between between time points in a panel nor between left and right panels.

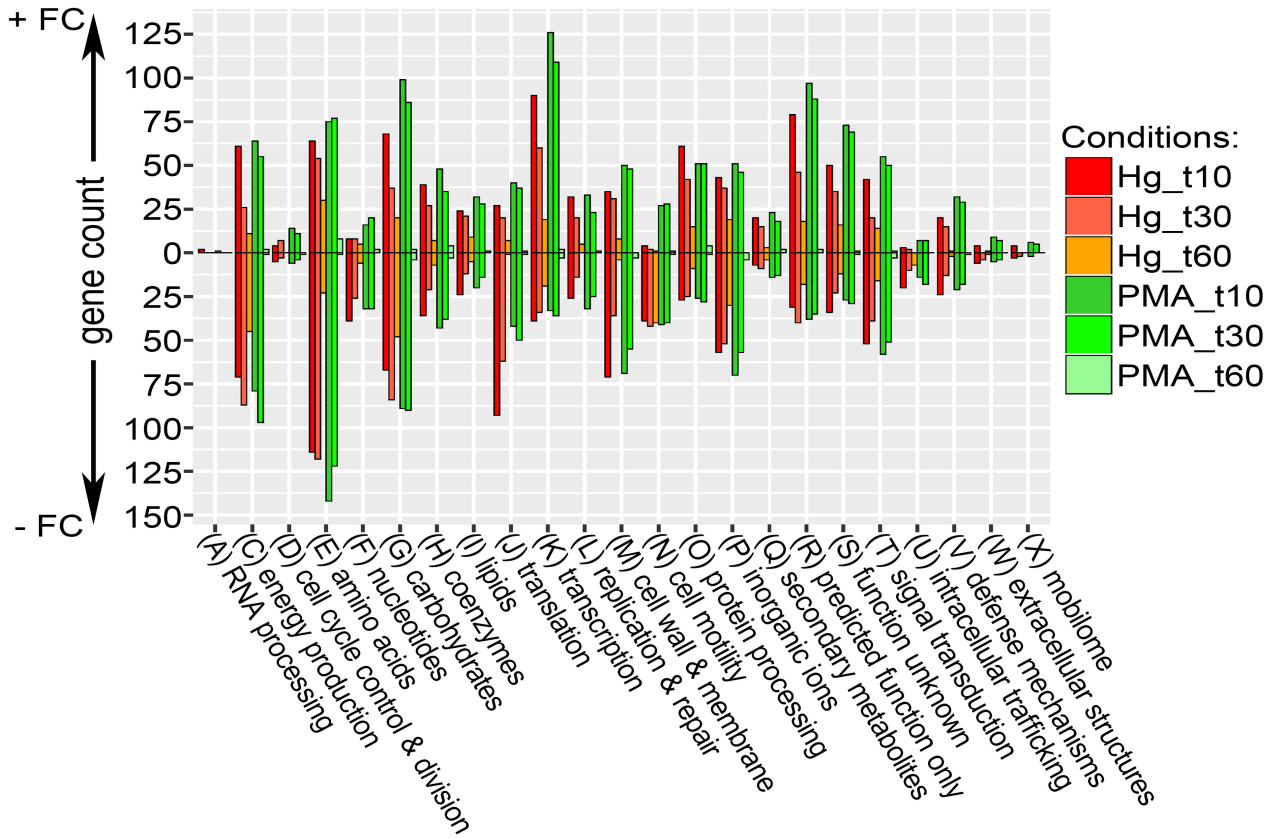

Figure 3: Counts of differentially expressed genes for each condition grouped by COG functional category. Genes with a $\log_2$ fold-change ≥ 1 for each condition were grouped by COG group. Positive counts represent observed up-regulated genes and negative counts represent observed down-regulated genes. COG code, number of proteins encoded by genome and category description: (A, 2) RNA processing and modification; (C, 284) Energy production and conversion; (D, 39) Cell cycle control, cell division, chromosome partitioning; (E, 355) Amino acid transport and metabolism; (F, 107) Nucleotide transport and metabolism; (G, 381) Carbohydrate transport and metabolism; (H, 179) Coenzyme transport and metabolism; (I, 121) Lipid transport and

metabolism; (J, 236) Translation, ribosomal structure and biogenesis; (K, 294) Transcription; (L, 139) Replication, recombination and repair; (M, 242) Cell wall, membrane and envelope biogenesis; (N, 102) Cell motility; (O, 156) Post-translational modification, protein turnover, chaperones; (P, 223) Inorganic ion transport and metabolism; (Q, 68) Secondary metabolites biosynthesis, transport and catabolism; (R, 261) General function prediction only; (S, 203) Function unknown; (T, 191) Signal transduction mechanisms; (U, 50) Intracellular trafficking, secretion, and vesicular transport; (V, 91) Defense mechanisms; (W, 31) Extracellular structures; (X, 60) Mobilome, prophages, transposons.

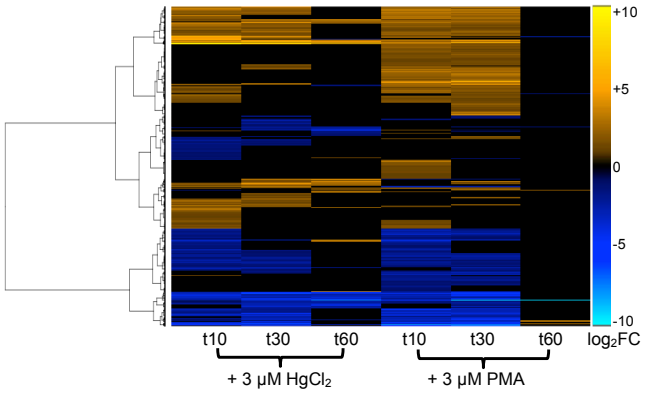

Figure 4: Differentially expressed genes at each RNA sampling time. Heat map of all genes that were differentially expressed in at least one mercury exposure condition (n = 3,149). Genes were clustered by row using Ward's minimum variance method [36] with non-squared $\log_2$ fold-change input values.

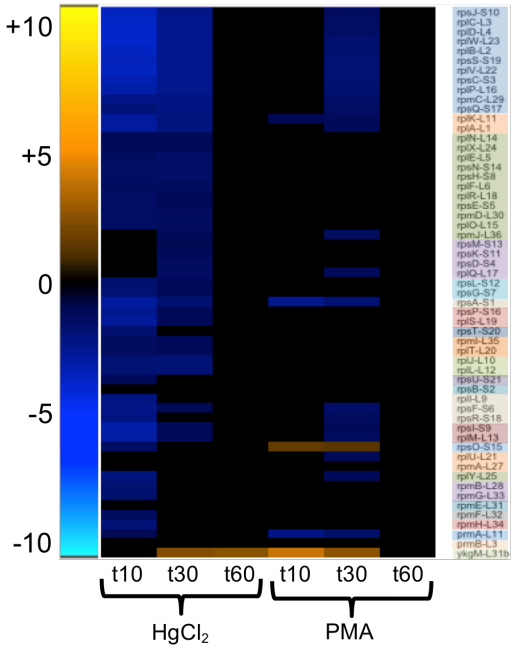

Figure 5: Ribosomal subunit protein genes. Genes are grouped and colored by operon (see larger Figure S11 and Table S13 for details).

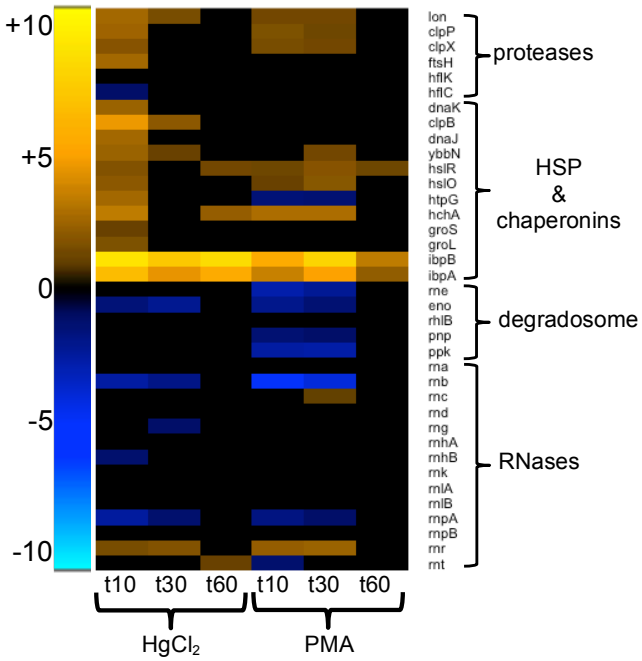

Figure 6: Protein and RNA turnover and repair. (see larger Figure S12 and Table S13 for details).

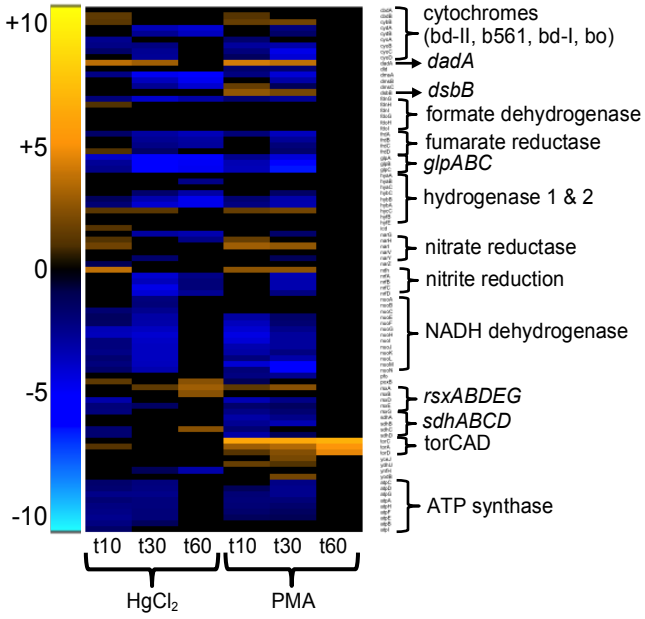

Figure 7: Electron transport chain and ATP-synthase. (see larger Figure S13 and Table S13 for details).

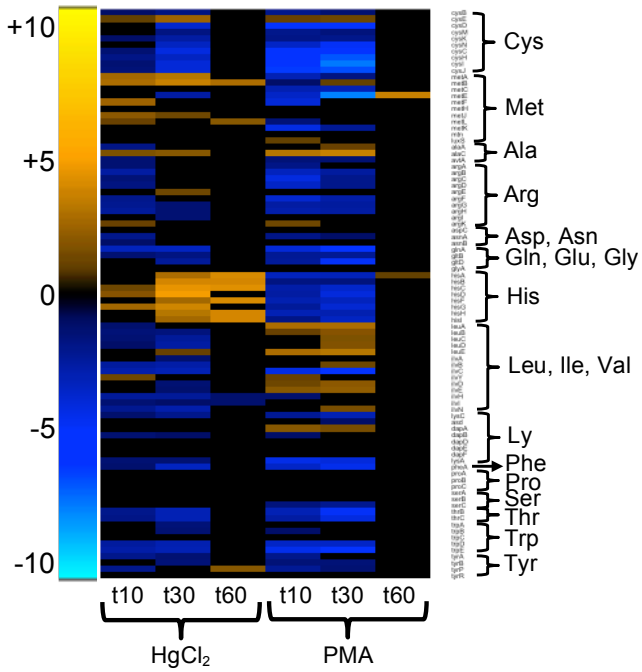

Figure 8: Amino acid biosynthesis. (see larger Figure S22 and Table S13 for details).

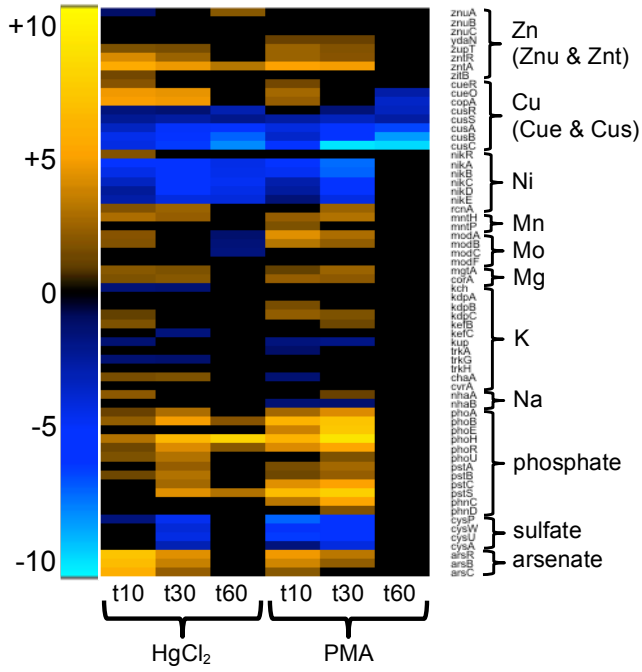

Figure 9: Non-ferrous metals homeostases. (see larger Figure S23 and Table S13 for details).

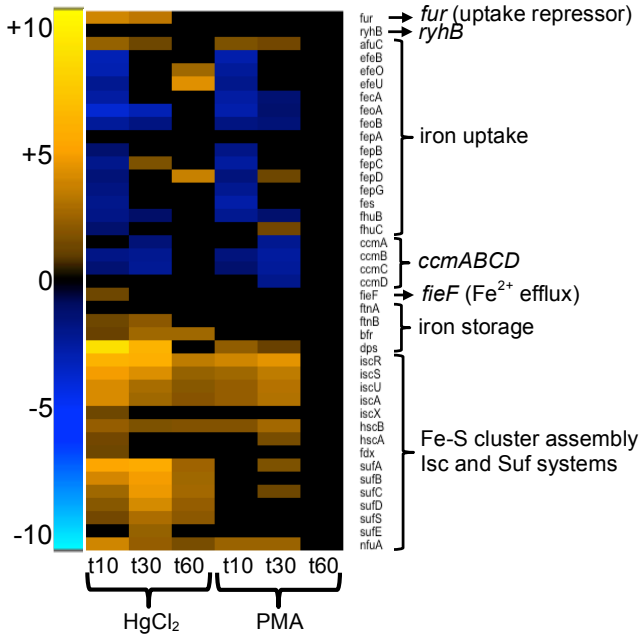

Figure 10: Iron homeostasis. (see larger Figure S24 and Table S13 for details).

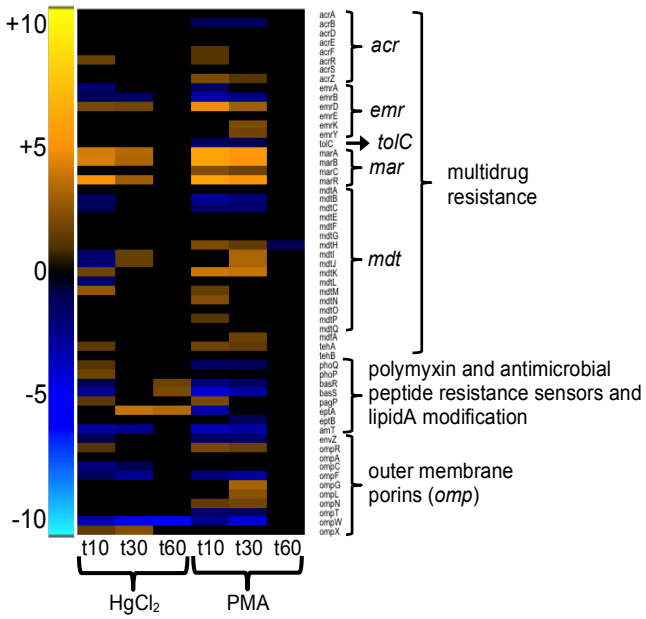

Figure 11: Antibiotic resistance and outer membrane porins. (see larger Figure S26 and Table S13 for details).

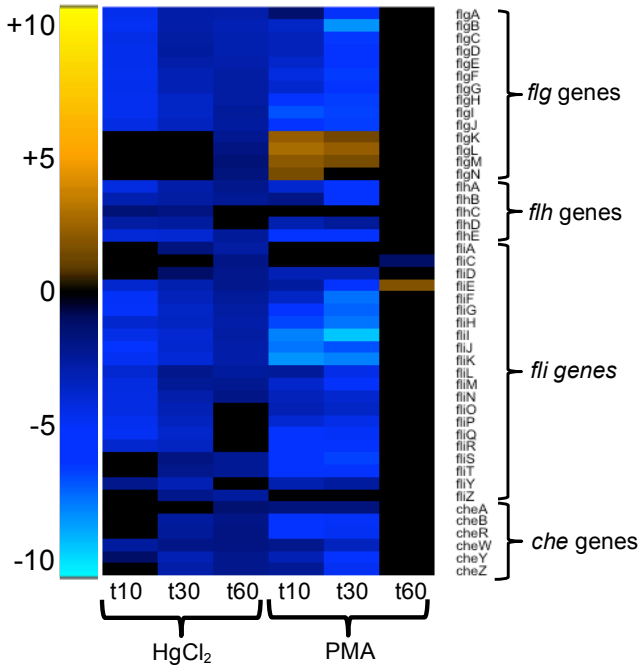

Figure 12: Flagella components and chemotaxis. (see larger Figure S27 and Table S13 for details).

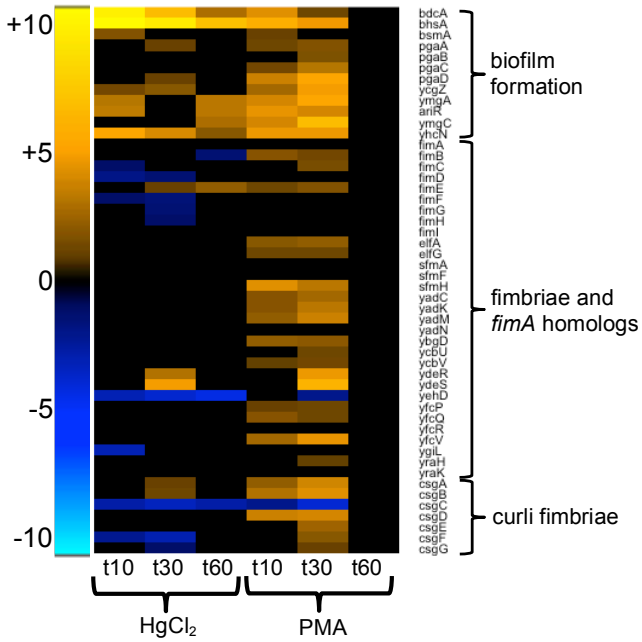

Figure 13: Biofilm formation and fimbriae. (see larger Figure S28 and Table S13 for details).

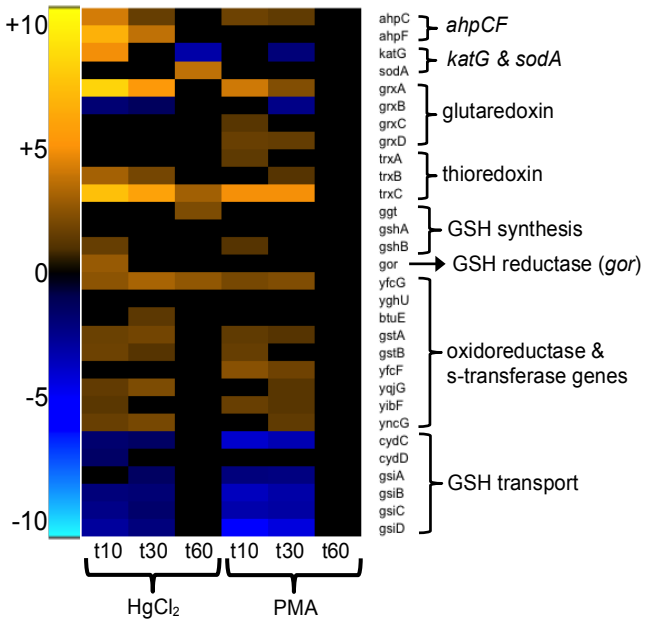

Figure 14: Oxidative stress defense and thiol homeostases. (see larger Figure S29 and Table S13).